Master of Science

CCR10-Mediated Enhancement of T Cell Trafficking for Improved Tumor Immunotherapy

The Graduate School

of the University of Ulsan of Medicine

Department of Medical Science

Jong Moo Hong

CCR10-Mediated Enhancement of T Cell Trafficking for Improved Tumor Immunotherapy

Supervisor: Hee Jin Lee

A Dissertation submitted to

the Graduate School of the University of Ulsan College of Medicine

In partial Fulfillment of the Requirement for the Degree of

Master of Science

by

Jong Moo Hong

Department of Medical Science

University of Ulsan College of Medicine, Korea

February 2024

CCR10-Mediated Enhancement of T Cell Trafficking for Improved Tumor Immunotherapy

This certifies that the master's thesis of

Jong Moo Hong is approved.

_____

Committee Chair Dr. Gyung yub Gong

_____

Committee Member Dr. Hee Jin Lee

_____

Committee Member Dr. Tae-Kyung Yoo

Department of Medical Science

University of Ulsan College of Medicine, Korea

February 2024

Acknowledgements

I would like to express my sincere gratitude to professor Hee Jin Lee, whose expertise and knowledge were invaluable in guiding and shaping this research.

Special thanks are extended to 정희원, 정성욱, 김지형, 한도연, 유성준, 김기범, 정성필, and 김도균 for their invaluable assistance and insightful critiques throughout the study.

I also wish to thank 이건희, 이인원, and 서정한 for their technical assistance, and 김영애 for their help in language editing and proofreading this manuscript.

Finally, I would like to extend my appreciation to my family and friends for their understanding and endless love, which was my greatest source of encouragement throughout this journey.

Contents

List of figures and tables

1. Materials & Methods

2. Result

3. Supplemental information

Abstract

The efficacy of adoptive T cell therapy is still not optimal for solid tumors, in part due to the insufficient T cell infiltration into the tumor site. An encouraging approach involves guiding T cells toward the tumor by utilizing tumor-specific chemokines, assuming that the corresponding chemokine receptor is present on the T cells. Analysis of RNA-seq data from TCGA and GTEx revealed high expression of the chemokine CCL28 in breast and lung cancer. However, the receptor for CCL28, CCR10 was found to have insufficient expression in human peripheral T cells, tumor-infiltrating T cells, and activated chimeric antigen receptors modified T cells (CAR-T). Hence, my goal was to utilize CCR10's potential to guide T cells to the tumor site and enhance the effectiveness of tumor immunotherapy. After expressing 1G4 in T cell receptor-engineered T cells (TCR-T), I employed cloning and lentivirus transduction to increase endogenous CCR10 expression. CCR10-1G4 dual expressing TCR-T exhibited comparable cellular cytotoxicity but demonstrated increased mobility *in vitro*. CCR10-1G4 dual expressing TCR-T injection to a xenograft tumor model exhibited enhanced *in vivo* trafficking and greater reduction of tumor burden in treated mice, compared to 1G4 TCR-T. This study not only elucidates the role of CCR10 in T-cell trafficking but also presents its potential for developing treatments targeting malignant tumors.

1. Introduction

Adoptive T cell therapy (ACT), also known as cellular immunotherapy, harnesses the power of tumor-specific T cells for cancer treatment (1). These T cells can be obtained directly from cancer patients as peripheral blood mononuclear cells (PBMCs) and tumor-infiltrating lymphocytes (TILs) or through engineering of T cells with a tumor antigen-specific T cell receptor (TCR) or a chimeric antigen receptor (CAR). The treatment of CAR-engineered T cells for hematological malignancy showed significant clinical success, which led to the approval of anti-CD19 CAR-T by the Food and Drug Administration in 2017, the first approved T cell therapy (2, 3). Although the anti-tumor effectiveness of CAR-T on solid tumors was demonstrated in preclinical models, efficiency was limited in clinical trials (3, 4). Until now, efforts to improve ACT in solid tumors have mainly been made to identify suitable antigens and CAR or TCR structures to enhance specificity and targeting (5). However, additional T-cell engineering and complex treatments have not shown meaningful clinical results so far (6).

One key impediment to the efficacy of ACT in solid tumors is the diminished T cell infiltration into tumor tissue (7). The T cells must interact with tumor cells to have an anti-tumor effect. If T cells do not have access to tumors, effective treatment cannot be done. The main causes of decreased T cell infiltration to tumor tissue include inefficient trafficking to the tumor area and difficult access to tumor cells through desmoplastic tumor stroma (8, 9, 10). Chemokines and their receptors have a significant impact on the movement of immune cells (11). They also have a crucial role in tumors by promoting tumor metastasis and invasion and generating an immune-resistant tumor microenvironment (12). Prior research has indicated that

these attributes of solid tumors can be leveraged to improve the migration of therapeutic T cells through the use of chemokine receptors (13). Introducing chemokine receptors that respond to tumor-derived chemokines can enhance the effectiveness of injected adoptive T cells.

To determine the optimal chemokine receptor for ACTs in breast cancer and lung cancer, I analyzed data from the Cancer Genome Atlas (TCGA) and The Genotype-Tissue Expression (GTEx). It revealed that the CCL28, which interacts with CCR10, is overexpressed in lung cancer and breast cancer compared to normal tissues. Furthermore, CCR10-expressing engineered T cells showed enhanced trafficking and anti-tumor effects *in vitro* and *in vivo*.

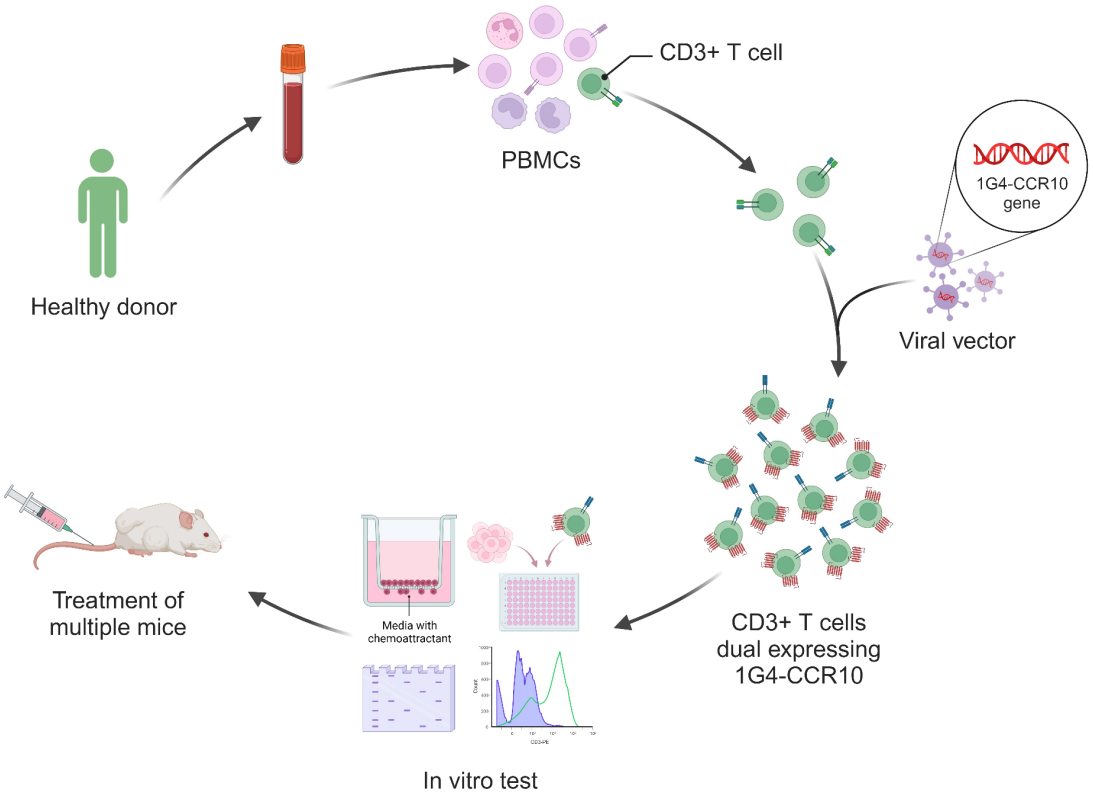

(Created in BioRender.com)

2. Materials and methods

2-1. Healthy blood samples

Healthy donor blood samples were obtained from an Asan Medical Center (IRB protocol 2017-0784). Blood was washed at a 1:1 ratio using DPBS containing 2% fetal bovine serum (FBS) (Gibco, NY, USA, #16000-044) after it was collected in BD Vacutainer® Heparin Tubes with Sodium Heparin (BD Vacutainer, UK, #REF 367874). PBMCs were obtained using Sepmate tubes (STEMCELL, Vancouver, Canada, #86450) and Lymphoprep (STEMCELL, #1858), and they were subsequently stored in CS10 (STEMCELL, #100-1061) buffer. The filled cryovials were placed in freezing containers at −80 °C for 24 h prior to transfer to liquid nitrogen for long-term storage. Prior to use, PBMCs were rested for one day in RPMI 1640 (Gibco, #22400-890) containing 10% FBS and 1% penicillin-streptomycin (Gibco, #15140122).

2-2. Cell line

Lenti-293X cells for virus packaging were purchased from ATCC (Virginia, USA). The human cancer cells Jurkat, A375, MDA-MB-231/436/468, MCF7, T47D, SKBR3 and SK-HEP-1 were obtained from ATCC. Jurkat, MDA-MB-231, MCF7, T47D and SKBR3 cells were cultured in RPMI 1640 medium (Gibco, #A10491-01) with 10% FBS and 1% penicillin-streptomycin. A375, Lenti-293X, MDA-MB-436/468 and SK-HEP-1 were cultured in DMEM (Gibco, #11995-065) with 10% FBS and 1% penicillin-streptomycin. After transduction, A375-Luc/CCL28 cells were cultured in DMEM with 10% FBS, 1% penicillin-streptomycin, puromycin (invitrogen, Waltham,

MA, USA, #ant-pr-1) and G418 (invitrogen, #ant-gn-1). All cancer cell lines were negative for mycoplasma using e-Myco™ Mycoplasma PCR detection kit (Lilif, Republic of Korea, #25235).

2-3. Isolation and expansion of TILs

Triple-negative breast cancer (TNBC) tissue was placed in RPMI 1640 medium and brought to the laboratory within 2 hours of surgery. After washing with RPMI containing gentamicin (Welgene, Gyeongsan-Si, Republic of Korea, #ML003-03), the tumor tissue was chopped into pieces with a diameter of 1 ~ 2 mm. The chopped pieces were placed in a 6 mL TIL culture [10% FBS and 1,000 IU/mL IL-2 (Miltenyi Biotec, Bergisch Gladbach, NRW, Germany, #130-097-748) in CTS™ AIM-V™ Medium, without phenol red, without antibiotics (Gibco, NY, USA, A3830801)] and seeded in a T75 flask. The plates were incubated at 37°C for 14 days to allow for further penetration and expansion of TILs from the tissue fragments. Half of the media were changed every two days. After the 14-days incubation period, a mixture of tissue pieces and TILs was passed through a strainer with 40 μm pores, followed by centrifugation at 1,500 rpm for 5 minutes to recover TILs. Subsequently, the TILs were counted and frozen (14).

For the rapid expansion of TILs, we employed the standard rapid expansion protocol as previously described (14), with a minor modification as follows: 5 × 10^4 TILs were cultured at 37°C in a T25 flask containing 3 mL of 50% RPMI 1640 and 50% AIM-V media supplemented with 3% human AB-serum (Sigma-Aldrich, St. Louis, MO, USA, #H3667), 1,000 IU/mL IL-2, 30 ng/mL human anti-CD3 antibody

(OKT3, Miltenyi Biotec, #130-093-377), and 1 × 10^7 irradiated (50 Gy) PBMC feeders. On day 4, 3 mL of the same media was added to the flask, and then 3 mL of media was added every 2 days. After 14 days, TILs (REP TILs) were collected, counted, and cryopreserved (15).

After preparing a library with the TruSeq Stranded mRNA Sample Prep Kit (Illumina, California, USA, #20020595) using REP-TIL samples from TNBC patients, we conducted RNA sequencing with 100 PE (paired end reads). Low-quality reads, adapter sequences, and reads shorter than 36 base pairs were removed from the raw data using Trimmomatic (version 0.38) (16). The reference for this process was obtained from the Illumina iGENOMES site. The paired.fastq file of clean reads was used for mapping to the Homo sapiens UCSC hg19 reference genome using STAR (version 2.6.0a) (17). The number of reads mapped to the reference was determined using RSEM (18), a tool for transcript quantification analysis. Differential expression gene (DEGs) analysis was conducted using FPKM, TPM, and Expected count from the output file. DEGs analysis was performed using R package DESeq2 (19).

2-4. Database tool and analysis / Chemokine and chemokine receptor detection

TCGA and GTEx data were used to compare the expression of each carcinoma, and Tumor and Normal transcription information were compared. TCGA provides multidimensional data for various carcinomas, including Blood Derived Normal samples and normal controls compared to cancer tissues from patients. Meanwhile, the GTEx database supplies gene expression and genotype data for normal tissues, including some cell line data. Tumor transcriptome expression data

were obtained from TCGA, and normal transcriptome data were obtained from GTEx. Breast cancer (N=1,075), lung adenocarcinoma (LUAD, N=576), lung squamous cell carcinoma (LUSC, N=552), analyses were performed using 7,788 in GTEx, respectively. The TPM value calculated using RSEM was used for the expression data, and data normalization was performed in the form of log2 (TPM+0.001) and compared.

The expression of chemokine receptors in CAR-T cells was analyzed using the Gene Expression Omnibus (GEO) database. Samples available in six GEO databases (GSE140107, GSE178570, GSE178998, GSE189932, GSE220927, and GSE218791) were selected and analyzed. If the gene value was missing (NA) in the selected samples, it was treated as 0 and included in the analysis. To ensure comparability among the six GEO databases, batch correction was performed using the combat method from the sva package in the R programming language.

2-5. The Design of TCR and CCR10 Expression Structures and the Generation of Target Cells

The coding DNA sequences (CDS) for CCR10 and CCL28 were obtained from the National Center for Biotechnology Information (NCBI). The CCR10 gene was extracted from PBMC using the Bioneer pfu pre-mix kit (Bioneer, Daejeon, Republic of Korea, K-2301) and primers (5'-atggggacggaggcc-3',5'-ctagttgtcccaggagagactg-3'). Subsequently, the CCR10 and 1G4 genes were cloned into the FUGW lentiviral vector (Addgene, Watertown, MA, USA, 14883). After purchasing the pCMV plasmid containing the CCL28 gene from the origene (Origene, Rockville, MD, USA, #RC209344), the CCL28 gene segment was amplified using PCR primers. Subsequently, it was cloned into the

pCDH vector (Addgene, #72266). Additionally, the Neomycin resistance gene was cloned to enable the selection of cells in which the CCL28 gene had been successfully transduced. Detailed primer information used is specified in Table 1. A375-Luc/CCL28 cells were generated through transduction using pCDH vectors containing the full-length human CCL28 gene and separate pCDH vectors containing the luciferase gene.

I used restriction enzymes Bmt1-HF (New England biolabs, #R3658), Kpn1-HF (New England biolabs, Ipswich, MA, USA, #R3142), Xma1-HF (New England biolabs, #R0180) and rCutSmart buffer (New England biolabs, #B6004S) in digestion processes. DNA purification used Gel extraction kit (QIAGEN, Hilden, Germany, #28704) and PCR purification kit (ThermoFisher, Waltham, MA, USA, #k310001). In ligation processes, I used Gibson Assembly Master Mix (New England Biolabs, #E2611). Mini prep kit (LaboPass, Seoul, Republic of Korea, #CMP0112) and Midi prep kit (MACHEREY-NAGEL, Dueren, Germany, #740422.50) + ligase (New England Biolabs, #M0202) for obtaining plasmids after Mini and Midi culture. RNase & DNase free-water were used as elution buffers (BioSolutions, Rockville, USA, #BW012). For checking the gene size, dilution buffers from 50x TAE buffer (Dyne bio, Seongnam, Republic of Korea, #CBT3020) to 0.5x TAE buffer were used. Dyen Agarose star (Dyne bio, DE100) was used to make 1% agarose gel. For electrophoresis, Dyne loading star (Dyne bio, A750), Dyne 1 kb Plus DNA ladder (Dyne bio, A738) were used.

Table 1. Primer sequences

Gene		Forward/Reverse	5'-3' Sequence
EF1α-1G4	EF1α-1G4	Forward	GGG CAG AGC CAC
		Reverse	CTATGAATTCTTTCTTTTGACCATAGCCA
	WPRE	Forward	AAT CAA CCT CTG GATTACA AAA TTT GTG
		Reverse	GGTACC GTGTGTGTG
EF1α-CCR10	EF1α-CCR10	Forward	GGG CAG AGC CAC
		Reverse	CTAGTTGTCCCAGGAGAGAC
	WPRE	Forward	AAT CAA CCT CTG GATTACA AAA TTT GTG
		Reverse	GGTACC GTGTGTGTG
EF1α-1G4 -CCR10	EF1α-1G4-T2A	Forward	ATAGCTAGCCGTGAGGCTCCGGTG
		Reverse	CCCCCCGGGTGGGCCAGGATTCTCCT
	CCR10-WPRE	Forward	CCCCCCGGGATGGGGACGGAGGCC
		Reverse	GGGGTACCCAGGCGGGGAGGC
EF1α-CCL28	CCL28	Forward	CGG GAT CCA TGG AGC AGA GAG GAC TCG
		Reverse	ACGCGTCGACTTAAACCTTATCGTCGTCATCCTTGT
	NeoR/KanR _SV40 promoter	Forward	CGGAATTCTCAGAAGAACTCGTCAA GAA GGC
		Reverse	GGGGTACCCGCGGAACCCCTATTTGTT

2-6. Viral particle preparation and TCR-T generation

Lenti-X 293T cells were cultured in DMEM with 10% FBS, 1% penicillin-streptomycin in T175 flask before doing transfection experiments. For the production of virus particles, lentiviral plasmid samples were employed in conjunction with a packaging vector (gag-pol, ENV, REV) and Lipofectamine 3000 Transfection reagent (Invitrogen, #L3000-075). After 2 days, the supernatant in the T175 flask was recovered and filtered by Millex 33 mm PES 0.45 um (Millipore, Burlington, MA, USA, #SLHPR33RS) and 50 cc syringe. The filtered samples were processed with the Lenti-X concentrator (Takara, Kusatsu, Japan, #631232) over a period of four days. Subsequently, all viral suspensions were prepared in RPMI 1640 (Gibco, #22400-089) and then aliquoted. To determine the viral concentration, p24 titration was conducted using the Lenti-X qRT-PCR Titration kit (Takara, #631235).

Prior to the introduction of PBMC, 2 X 10^7 PBMCs were activated using 100 μl of T cell TransAct human (Miltenyi Biotec, #130-111-160) and 20 IU/ml of IL-2 (Miltenyi Biotec, #130-097-748) for 2 days in a T25 flask. The transduction process was carried out to create 1G4 T cells, CCR10 T cells, and CCR10-1G4 dual expressing TCR-T cells. After seeding 2 X 10^6 cells into a 6-well plate, lentiviruses were mixed together, 30 mg/ml of protamine was added, and then the mixture was centrifuged at 800g for 2 hours at 32℃. Following centrifugation, the medium was changed to RPMI 1640 supplemented with 400 IU/ml of human IL-2 every 2 days after transferring the cells to a T25 flask. FACS analysis was also performed on days 8, 10, and 12 to verify the expression of 1G4 and CCR10. The Jurkat cell transduction was performed in the same way except for the activation process.

2-7. *In vitro* Transwell assay

To evaluate the migratory efficiency of T cells, I employed a Transwell assay utilizing a 24-well plate and 6.5 mm Transwell inserts with a pore size of 5.0 μm (Corning, NY, USA, #3421)(20). PBMCs were seeded at a density of 5 x 10^6 cells in the upper chamber, while the lower chamber was filled with chemotaxis buffer (0.1% BSA in RPMI 1640) supplemented with recombinant human CCL28 protein (R&D, MN, USA, #717-vc-025/CF). The assay was conducted within a CO2 incubator for a duration of 2 hours to facilitate cell migration. Subsequent to the incubation period, all the buffer from the lower chamber was meticulously collected into FACS tubes(Falcon, London, UK, #352052) and combined with 100 μl of precision count beads (BioLegend, San Diego, California, USA, #424902). The ratios were then computed using FACS data in accordance with the precision count beads protocol.

$$Absolute\ Cell\ Count\ \left({}^{Cells}/_{\mu L}\right) = \frac{Cell\ Count\ X\ Precision\ Count\ Beads™\ Volume}{Precision\ Count\ Beads™\ Count\ X\ Cell\ Volume}\ x\ Precision\ Count\ Beads\ ™\ Concentration\ \left({}^{Beads}/_{\mu L}\right)$$

2-8. Western blot

For checking migration signaling, cells expressing 1G4 or 1G4-CCR10 incubated in the RPMI 1640 with recombinant human CCL28 protein for 0, 5, 10 and 15 minutes. Then, the washing process was carried out with DPBS. To extract proteins in the cells, RIPA buffer which was added 1 mM PMSF (Cell signaling technology, Danvers, MA, USA, #9806) and incubated for 5 minutes in the ice, was used. After centrifugation 14,000 G for 10 minutes in the 4℃, a supernatant with extracted proteins was obtained. The amount of protein to use was quantified via BCA Protein assay kit (ThermoFisher, #23227). After quantifying the extracted

protein, it was mixed with 4X Bolt™ LDS Sample Buffer (Invitrogen, #B0007). The prepared samples, along with SeeBlue™ Plus2 Pre-stained Protein Standard (Invitrogen, #LC5925), were loaded onto BOLT BISTRIS PLUS 4~12% 12 Well gels (Invitrogen, #NW04122BOX). Membrane transfer was carried out using IBLOT NC GEL TRANSFER STACKS Regular (Invitrogen, #IB23001) and the iBlot™ 2 Gel Transfer Device (Invitrogen, #IB21001). For the transfer buffer, 10X TRIS-GLYCINE BUFFER (W/O SDS) (Biosesang, Cheoin-gu, Republic of Korea, #TR2028-100-00) along with Methanol (Supelco, #1.06009.1011) was used.

To check migration signaling, p44/42 MAPK (Erk1/2) antibody, Phospho-p44/42 MAPK (Erk1/2)(Tyr202/Tyr204) antibody, Akt antibody, and Phospho-Akt (Ser473) antibody (Cell signaling technology, #9101, #9102, #9271, #9272) was used. All primary antibodies used were diluted to a 1:1000 concentration, while the Rabbit IgG (H+L) secondary antibody HRP was diluted to a 1:5000 concentration as the secondary antibody. After antibody treatment, the reaction was initiated by treating it with Dyne ECL STAR (DYNE BIO, #DN-250).

2-9. Cytotoxicity assay *in vitro* and cytokine measurements

To ascertain the equivalence in killing ability between 1G4 TCR-T and CCR10-1G4 dual expressing TCR-T, a cytotoxicity assay was performed using luciferase-labeled target cells. T cells and A375-Luc/CCL28 target cells were seeded at a density of 3 x 10^4 cells per well. Co-cultures were established in 96-well plates with a total volume of 100 μl media, maintaining effector-to-target E/T ratios of 1:1, 3:1, 10:1, and 30:1. After a 24-hour incubation period, the Bright-Glo™ Luciferase Assay kit(Promega, WI, USA, #E2620) was used to add 100 μl of luciferase reagent to each well, followed by a 5-minute incubation before measuring the luminescence

signal. The percentage of cell death was calculated according to the following formula: Cell death% = (Experimental Luciferase Release (OD450) − Target Cell Alone Blank (OD450))/(Triton-X-100 treated target cell luciferase release (OD450) − Target Cell Alone Blank (OD450)) x 100. Human IFN-γ and IL-2 from a cell culture supernatant were measured by an Human IFN-γ enzyme-linked immunosorbent assay (ELISA) kit (komabiotech, Yeongdeungpo-gu, Republic of Korea, #K0331121) and IL-2 Human Uncoated ELISA Kit (ThermoFisher, #88-7025-88) following the manufacturer's instructions.

2-10. Xenograft tumor model and *in vivo* functional assessment.

NOD.CB17-Prkdc scid/NCrKoat mice were procured from koatech (Pyeongtaek, Republic of Korea). For the A375 xenograft tumor model, 3 × 10^6 A375-Luc/CCL28 cells were subcutaneously (s.c.) injected into NOD-SCID mice. Tumor growth was monitored through bioluminescence imaging with the IVIS Imaging System and direct measurement of tumor size. Four days after tumor inoculation, the mice were divided into three groups, and each group received an intravenous injection of DPBS Control, 1 × 10^7 1G4 TCR-T, and CCR10-1G4 dual-expressing TCR-T. Analysis of the IVIS data was performed using Living Image software (PerkinElmer, Waltham, MA, USA). After labeling the T cells with IVISense DiR 750 Fluorescent Cell Labeling Dye (PerkinElmer, #125964), their bio-distributions at different time points 24, 48 and 72 hours post-injection were assessed. Quantification was performed using Living Image software (PerkinElmer). Tumor load was subsequently assessed at intervals of 3~4 days, and for quantification purposes, specific tumor regions were chosen, and the total

bioluminescence signals were measured using the IVIS Imaging System software. All mouse experiments were conducted in accordance with the guidelines of the Animal Welfare and Handling Guidelines and were approved by Asan Medical Center IACUC (Institutional Animal Care and Use Committee).

2-11. Flow cytometry

Fluorescence-activated cell sorting (FACS) was performed to check the expression of the transduced PBMCs. After Fc blocking using Human TruStain FcX (Biolegend, #422302) for 5 min at RT, transduced PBMCs were incubated with antibodies for 20 min at 4℃ in the dark. The monoclonal antibodies (mAbs) used to examine the expression of indicated proteins were purchased from the following vendors: (1) BioLegend: allophycocyanin (APC)-Cyanine7 (Cy7) anti-human CD3 (#300318), fluorescein isothiocyanate (FITC) anti-human CD4 (#300506), PerCP/Cy5.5 anti human CD8a (#301032) and PE anti-mouse TCR β chain (#109208). (2) BD Pharmingen (San Jose, CA, USA): APC-mouse anti-human CCR10 (#564771). PBMCs were washed and resuspended with FACS buffer by 2 times. The cells were centrifuged at 4℃ for 5 min and resuspended with DAPI (Invitrogen, #D3571). Data were acquired on a FACSCanto 2 device (BD Biosciences) and analyzed by FlowJo version 10.8.1 (Tree Star).

2-12. Statistical analysis

All Western Blot results are normalized to internal control gene beta actin. For the assessment of cytotoxicity and migration capability of both 1G4 TCR-T and

CCR10-1G4 dual expressing TCR-T *in vitro*, three technical replicates were executed within the same experiment. The data are presented as the mean ± SD of these three technical replicates, and a minimum of three independent experiments were carried out. Significance analysis was performed using two-way ANOVA, with significance levels denoted as follows: *p < 0.05, **p < 0.01, ***p < 0.001, ****p < 0.0001. The unpaired T-test was employed for the calculation of p-values. Standard curve regression analyses were conducted with GraphPad Prism (GraphPad Software, La Jolla, CA, USA). The data are expressed as mean ± SD unless specified otherwise. FlowJo software (Tree Star, USA) was employed for the analysis of all cytometric assays.

3. Results

3-1. Expression of CCL28 in Breast tumor, LUAD, and LUSC.

The conditions for selection of optimal chemokine receptors for adoptive T cell therapy include 1) higher expression of corresponding chemokines in tumor tissue than normal tissue in the body and 2) lower expression of chemokine receptors in activated T cells. To identify chemokines which are highly expressed in tumor tissue compared to normal, we analyzed TCGA and GTEx data.

Among the low-expression chemokine ligands in the GTEx normal dataset, I focused on CCL28, which has not yet been extensively studied. It was confirmed that the expression of CCL28 in TCGA data for Breast cancer, LUAD, and LUSC was higher than the expression levels observed in the GTEx normal dataset (Fig. 1A). Furthermore, when comparing TCGA and GTEx data for various chemokine ligands and listing them in order of the largest difference in expression, CCL28 exhibited a substantial difference in expression (Supplemental information table). Of the 58 chemokine ligands, Breast cancer had the 17th highest level of expression, LUSC had the 22nd, and LUAD had the 20th highest level of expression.

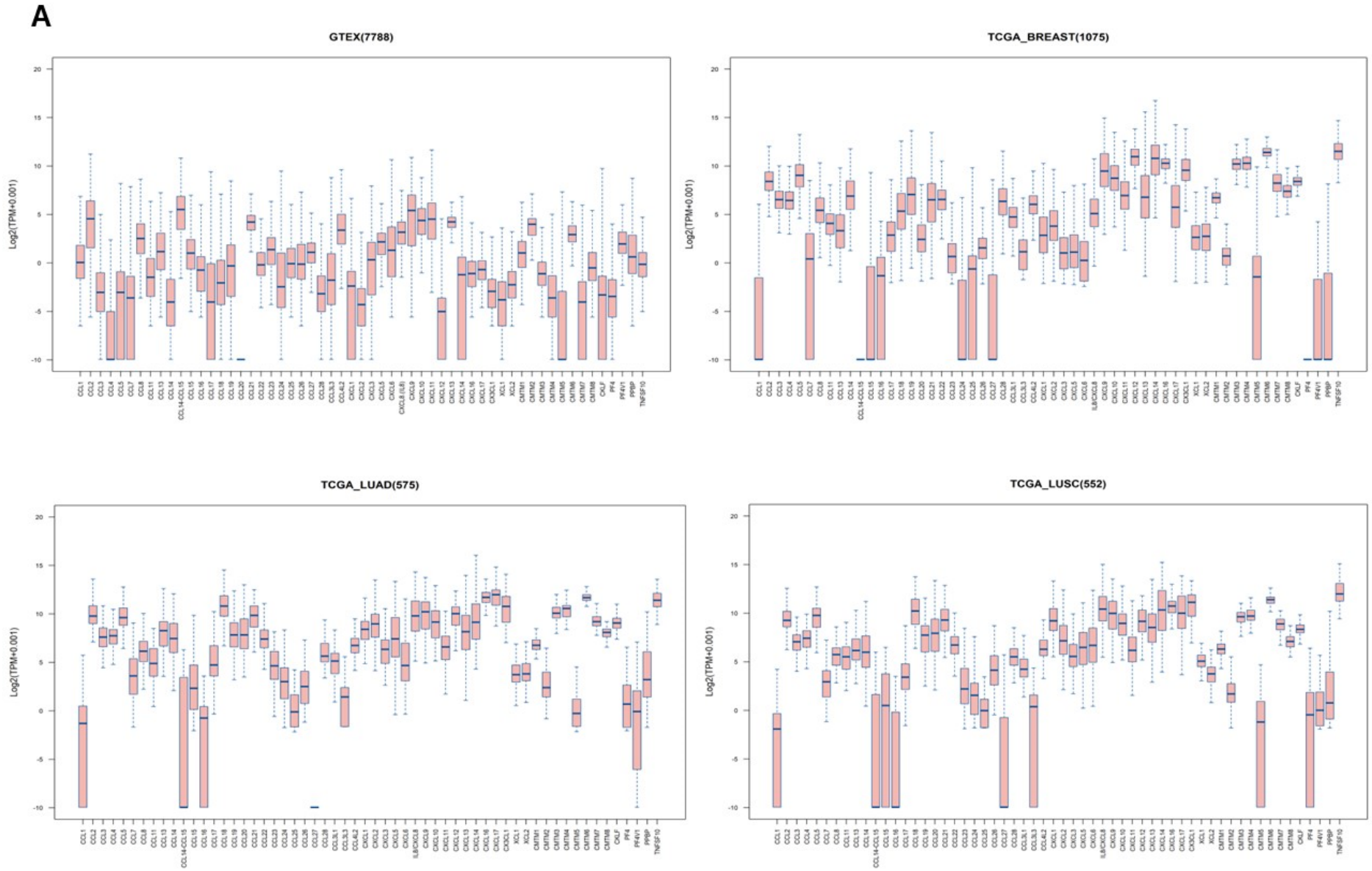
A
GTEX(7788)
TCGA_BREAST(1075)
TCGA_LUAD(575)
TCGA_LUSC(552)
Log2(TPM+0.001)

Figure1.

Chemokine expression profile in BRC, LUAD and LUSC. (A) The expression of 59 chemokine ligands in patients with BRC (n = 1075), LUAD (n = 575), and LUSC (n = 552) was analyzed using the online databases of TCGA and GTEx. Error bars represent mean ± SD.

3-2. Human peripheral T cells, CAR-T, and TILs lack expression of CCR10

Several types of chemokines are found in the tumor microenvironment, but corresponding chemokine receptors may not be expressed in effector T cells. Therefore, I investigated the chemokine receptors expressed in TILs, CAR-T, and peripheral CD3+ T cells. First, I analyzed RNA-seq data from the GEO database to verify changes in the expression of CCR10 in CAR-T (Fig. 2A). Expression levels were low for the receptors CCR10, CCR3, CCR9, CXCR2, CXCR5, and XCR1. Using RNA-Seq, I quantitatively analyzed RNA expression of chemokine receptors in cultured REP TILs. Among the several analyzed receptors, the RNA expression levels of CCR10, CXCR5, ACKR2, and ACKR3 were found to be low (Fig. 2B). In addition, RT-PCR was performed to confirm expression of chemokine receptors for TILs, Jurkat cells, and peripheral CD3+ T cells from breast cancer patients. All three types of cells exhibited low expression of CCR10 and several other chemokine receptors, similar to the RNA-seq data mentioned above (Fig. 2C).

Based on these results, I selected CCR10 as a potential candidate gene to be engineered in TCR-T to enhance homing and anti-tumor efficacy. I used FACS to assess CCR10 expression in activated human T cells, aiming to investigate the precise CCR10 expression in peripheral T cells while considering the potential modulation of chemokine receptor expression following T cell activation. After activation, CCR10 exhibited an initial increase on day 4, followed by a subsequent decrease in expression (Fig. 2D).

A

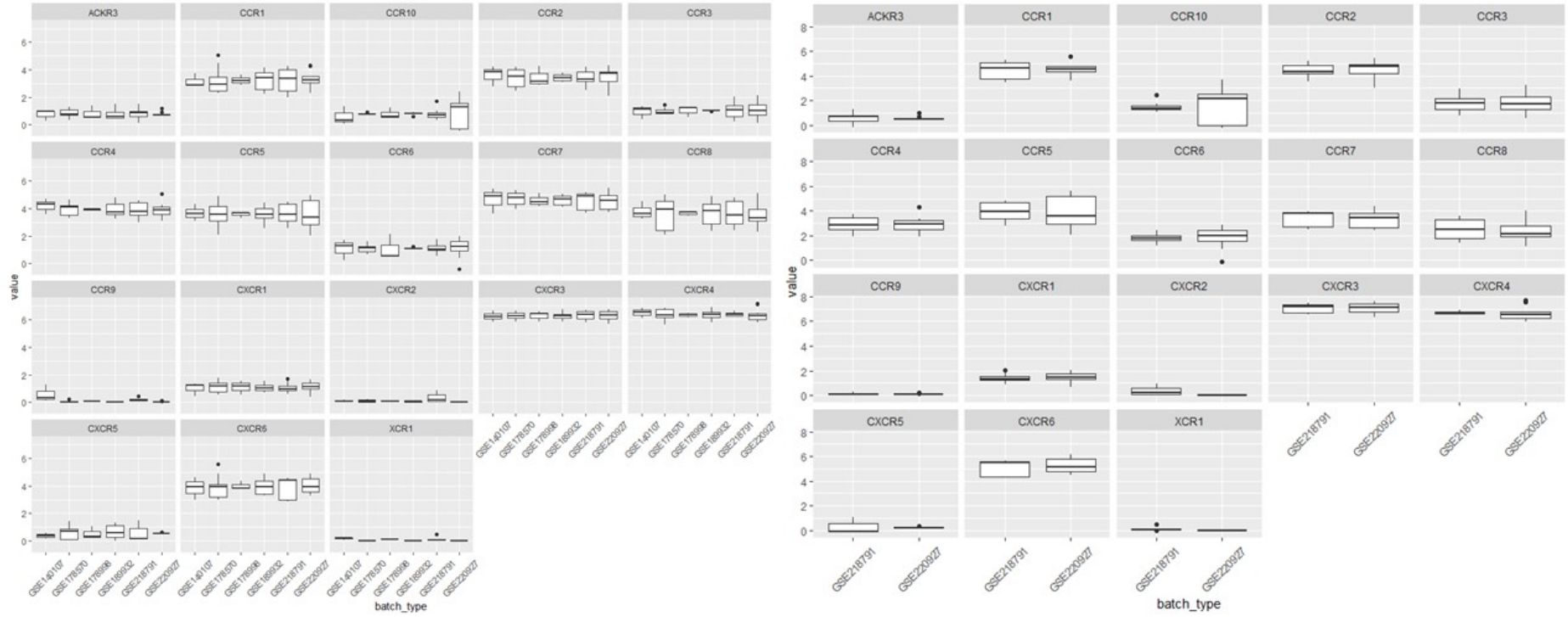
ACKR3
CCR1
CCR10
CCR2
CCR3
CCR4
CCR5
CCR6
CCR7
CCR8
CCR9
CXCR1
CXCR2
CXCR3
CXCR4
CXCR5
CXCR6
XCR1
value
batch_type
GSE140107
GSE178570
GSE178998
GSE169032
GSE218791
GSE220927

B

#	Chemokine receptor	Normalized log2 (FPRM+0.001) Mean	SD
1	CCR1	5.002	0.758
2	CCR2	5.994	0.678
3	CCR3	4.236	1.242
4	CCR4	4.190	0.766
5	CCR5	7.054	0.466
6	CCR6	3.252	0.464
7	CCR7	1.698	1.260
8	CCR8	3.601	0.863
9	CCR10	-1.472	2.177
10	CXCR1	2.615	0.493
11	CXCR3	7.278	0.485
12	CXCR4	8.196	0.427
13	CXCR5	-2.977	1.485
14	CXCR6	5.493	0.719
15	CX3CR1	2.346	0.834
16	ACKR2	-2.171	1.121
17	ACKR3/CXCR7	-0.053	0.465
18	CCRL2	2.065	0.451

C

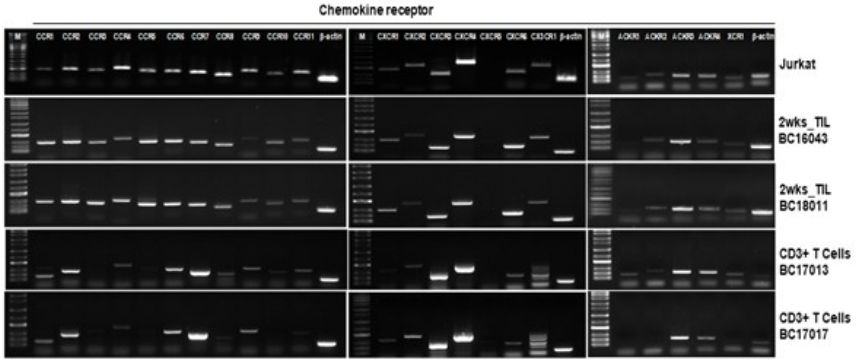

D

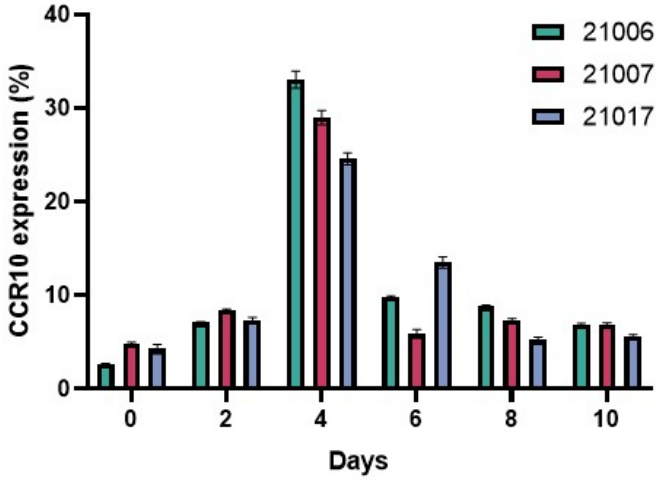

Figure 2

Profile of Chemokine Receptor Expression in CAR-T, TILs, and PBMC CD3+ T Cells. (A) Chemokine receptor expression levels in CAR-T cells were determined using RNA-seq data from the GEO database, which was subsequently modified using the R programming language's sva package. (B) RNA sequencing was conducted on 14 samples of TNBC TILs, and the expression levels of chemokine receptors were quantified in terms of normalized FPKM values. (C) Chemokine receptors were assessed in Jurkat cells, 2-week-old TILs, and CD3+ T cells via PCR analysis. (D) Following PBMCs activation, the expression of CCR10 was monitored via flow cytometry (FACS) every 2 days. Data represents mean ± SD.

3-3. Selection of a target cell line that reacts with CCR10

The target cell line chosen for this study was the melanoma cell line A375, which has HLA-A*02:01 and expresses NY-ESO-1, a peptide known to interact with the 1G4 TCR, a receptor that has been extensively studied previously (21). RT-PCR was conducted using the NY-ESO-1 primer to directly assess the expression of the NY-ESO-1 in A375 cells. NY-ESO-1 expression was observed in A375 cells, with slight expression also detected in the T47D cell line (Fig. 3A)

The level of CCL28 expression was quantitatively measured using ELISA, which is a corresponding chemokine of CCR10. In addition to the A375 cell line, other cell lines were also analyzed. ELISA showed that CCL28 was not detected in A375 but detected in breast cancer cell lines MDA-MB-468 and T47D (Fig. 3B). Since CCL28 was not secreted in the A375, which was selected as the target, we proceeded with CCL28 overexpression. To quantify the level of CCL28 expression after transduction, an ELISA test was conducted to assess whether there were differences in expression over time and with varying cell numbers. In addition, CCL28 was measured in culture media of A375 and A375-CCL28 cell lines that were cultured for two days at T175 flask. CCL28 increased as the number of cells and time increased (Fig. 3C).

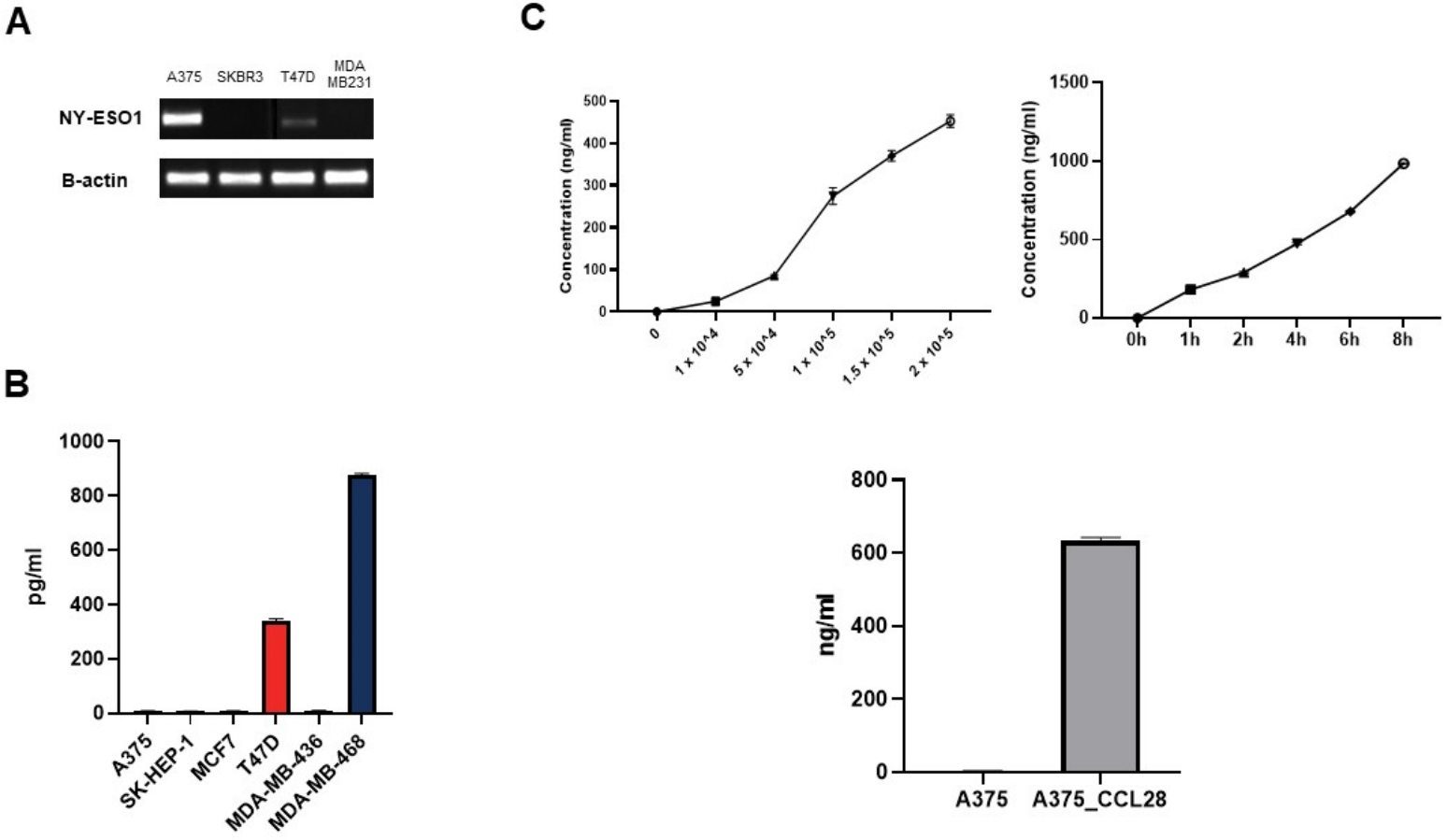
A
A375
SKBR3
T47D
MDA MB231
NY-ESO1
B-actin
B
pg/ml
1000
800
600
400
200
0
A375
SK-HEP-1
MCF7
T47D
MDA-MB-436
MDA-MB-468
C
Concentration (ng/ml)
500
400
300
200
100
0
0
1 x 10^4
5 x 10^4
1 x 10^5
1.5 x 10^5
2 x 10^5
Concentration (ng/ml)
1500
1000
500
0
0h
1h
2h
4h
6h
8h
ng/ml
800
600
400
200
0
A375
A375_CCL28

Figure 3

Chemokine expression profile in cancer cell lines. (A) The expression level of the NY-ESO-1 peptide in the cancer cell line was detected using RT-PCR. Representative data from one of the three replicate experiments are shown. (B) CCL28 secretion in cancer cell lines (*n* = 3) (C) CCL28 secretion was measured after lentiviral vector transformation in the A375 cell line. Data represents mean ± SD.

3-4. After engineering T cells with the 1G4 T cell receptor and CCR10 chemokine receptor, we conducted a promoter test

To co-express 1G4 TCR and CCR10 in T cells, I first explored methods for enhancing their expression efficiency. I conducted a comparison of the efficiency between the EFS promoter and the EF1α promoter (Fig. 4A). I constructed different structures by placing each promoter upstream of the 1G4-CCR10 genes. After transduction into Jurkat cells, the degree of expression was measured on day 12 of culture. When using the EF1α promoter, CCR10 expression was higher compared to when using the EFS promoter (Fig. 4B). To assess the extent of transferred gene expression during cell proliferation, gene expression was measured on days 0, 6, and 12 after sorting Jurkat cells expressing CCR10. The expression of the CCR10 gene with the EFS promoter decreased more over time compared to the EF1α promoter (Fig. 4C). Therefore, EF1α promoter was chosen for the further study.

1G4 and 1G4-CCR10 were transduced into the PBMC derived T cells of healthy donors and Jurkat cells (Fig. 4D). The co-expression level of 1G4 TCR and CCR10 in Jurkat cells was 43.5%, and the degree of expression in genetically modified T cells varied depending on the PBMC donors, with a range of expression from 13% to 36% (Fig. 4E).

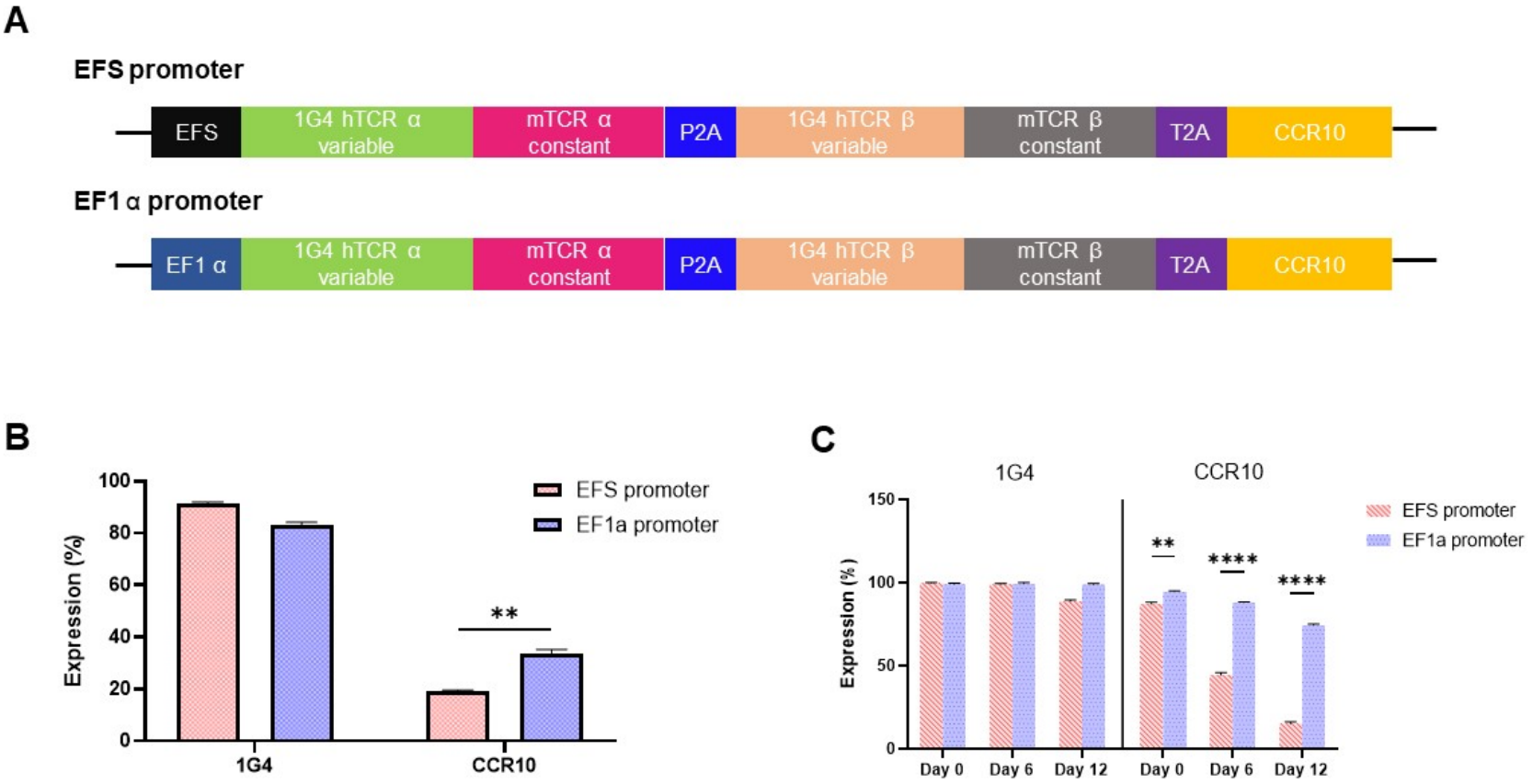
A
EFS promoter
EFS
1G4 hTCR α variable
mTCR α constant
P2A
1G4 hTCR β variable
mTCR β constant
T2A
CCR10
EF1 α promoter
EF1 α
1G4 hTCR α variable
mTCR α constant
P2A
1G4 hTCR β variable
mTCR β constant
T2A
CCR10
B
Expression (%)
100
80
60
40
20
0
EFS promoter
EF1a promoter
**
1G4
CCR10
C
1G4
CCR10
Expression (%)
150
100
50
0
EFS promoter
EF1a promoter
**
****
****
Day 0
Day 6
Day 12
Day 0
Day 6
Day 12

D

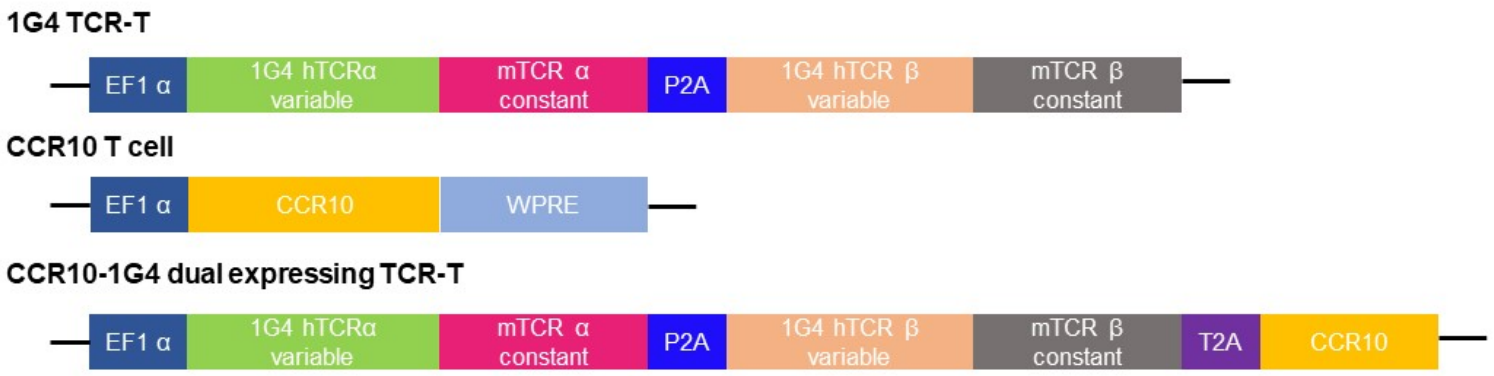
1G4 TCR-T
EF1 α
1G4 hTCRα variable
mTCR α constant
P2A
1G4 hTCR β variable
mTCR β constant
CCR10 T cell
EF1 α
CCR10
WPRE
CCR10-1G4 dual expressing TCR-T
EF1 α
1G4 hTCRα variable
mTCR α constant
P2A
1G4 hTCR β variable
mTCR β constant
T2A
CCR10

E

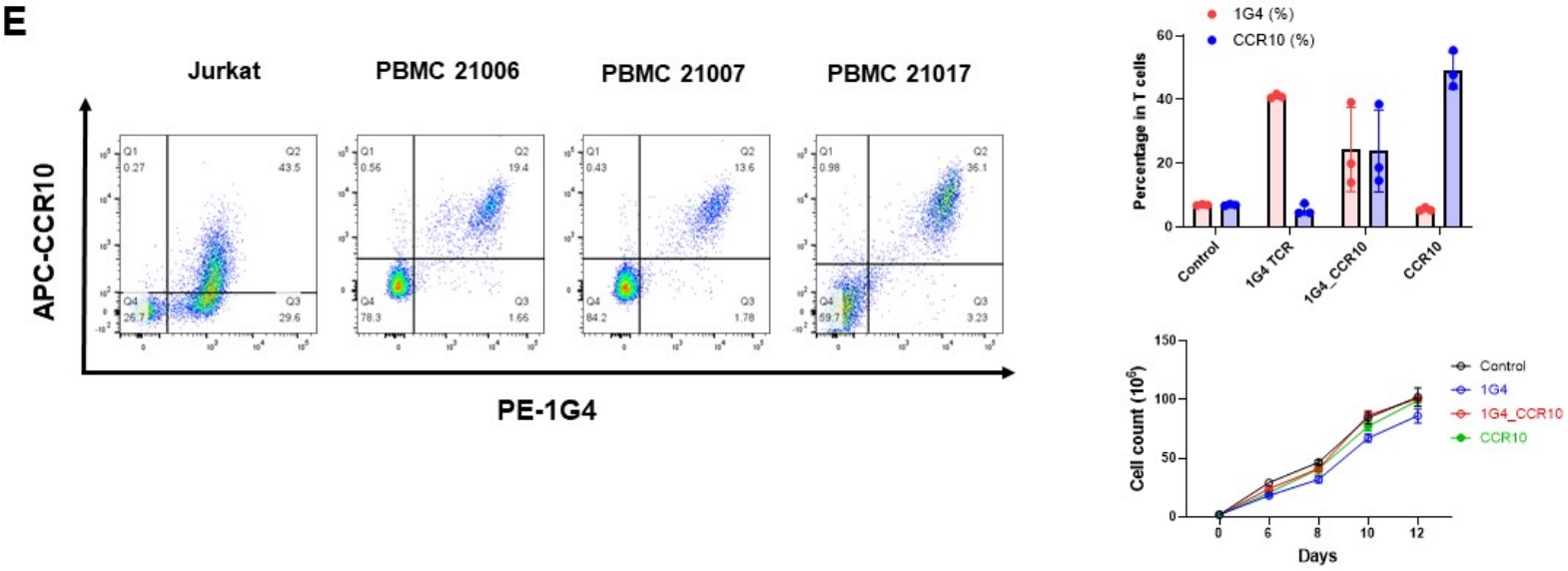
Jurkat
PBMC 21006
PBMC 21007
PBMC 21017
APC-CCR10
PE-1G4
Q1 0.27
Q2 43.5
Q4 26.7
Q3 29.6
Q1 0.56
Q2 19.4
Q4 78.3
Q3 1.66
Q1 0.43
Q2 13.6
Q4 84.2
Q3 1.78
Q1 0.98
Q2 36.1
Q4 59.7
Q3 3.23
1G4 (%)
CCR10 (%)
Percentage in T cells
Control
1G4 TCR
1G4_CCR10
CCR10
Cell count (10^6)
Days
Control
1G4
1G4_CCR10
CCR10

Figure 4

The specificity of NY-ESO-1 recognition by 1G4 and the construction of CCR10-1G4 dual expressing TCR-T. (A) To measure the expression difference based on promoters, the EFS promoter and EF1α promoter were attached differently before the CCR10-1G4 gene. (B,C) The expression of transgenes in lentivirus-transduced T cells was analyzed by flow cytometry using anti-mouse TCR β chain antibody and anti-human CCR10 antibody. (B) The expressions of 1G4 and CCR10 were measured 12 days after the transduction of Jurkat. (C) After sorting the transduced Jurkat cells, the expression measurement was conducted on days 6 and 12. (D) EF1α promoter was attached to CCR10-1G4 dual expressing TCR-T and 1G4 TCR-T. (E) Cell harvesting was performed on the 12th day of culture, followed by flow cytometry measurements. Each dot represents an individual sample (n = 3). Data represents mean ± SD. Two-way ANOVA was conducted for statistical analysis. ** $p < 0.01$, ****$p < 0.0001$.

3-5. When CCR10 is expressed, migration of CCR10 TCR-T is promoted

In order to assess the influence of CCR10 transduction on T cell migration, I conducted a transwell assay. (Fig. 5A). After incubation at 37°C, I counted the migrated T cells from the bottom chamber and analyzed the migration percentage. Migration efficiency ranged from 4.13% to 8.66% at 600 ng concentration of CCL28 and from 5.58% to 15.94% at 1,200 ng concentration. This demonstrated a notable increase in migration efficiency compared to T cells expressing only the 1G4 TCR (form 1.17% to 5.13% at 600 ng, from 1.28% to 10.65% at 1200 ng) (Fig. 5B). Notably, extending the incubation time had no substantial effect on trafficking efficiency, this indicates that migration driven by chemokine ligands is an initial process (Fig. 5C). Subsequently, a Western blot analysis was performed to identify the activation of the chemokine receptor signaling. Erk and Akt were chosen from the signaling mediators within the migration signaling pathway. Following exposure to the CCL28, phosphorylated forms of Erk and Akt were observed in T cells expressing both 1G4 and CCR10. Furthermore, it was shown that the Erk and Akt phosphorylation decreased over time during incubation, suggesting that the migratory response is an early event (Fig. 5D).

These findings illustrated that CCR10 can substantially boost the *in vitro* migratory capacity of 1G4 TCR-T, and the chemokines released by A375-Luc/CCL28 cells were capable of stimulating the migration of CCR10-1G4 dual-expressing TCR-T.

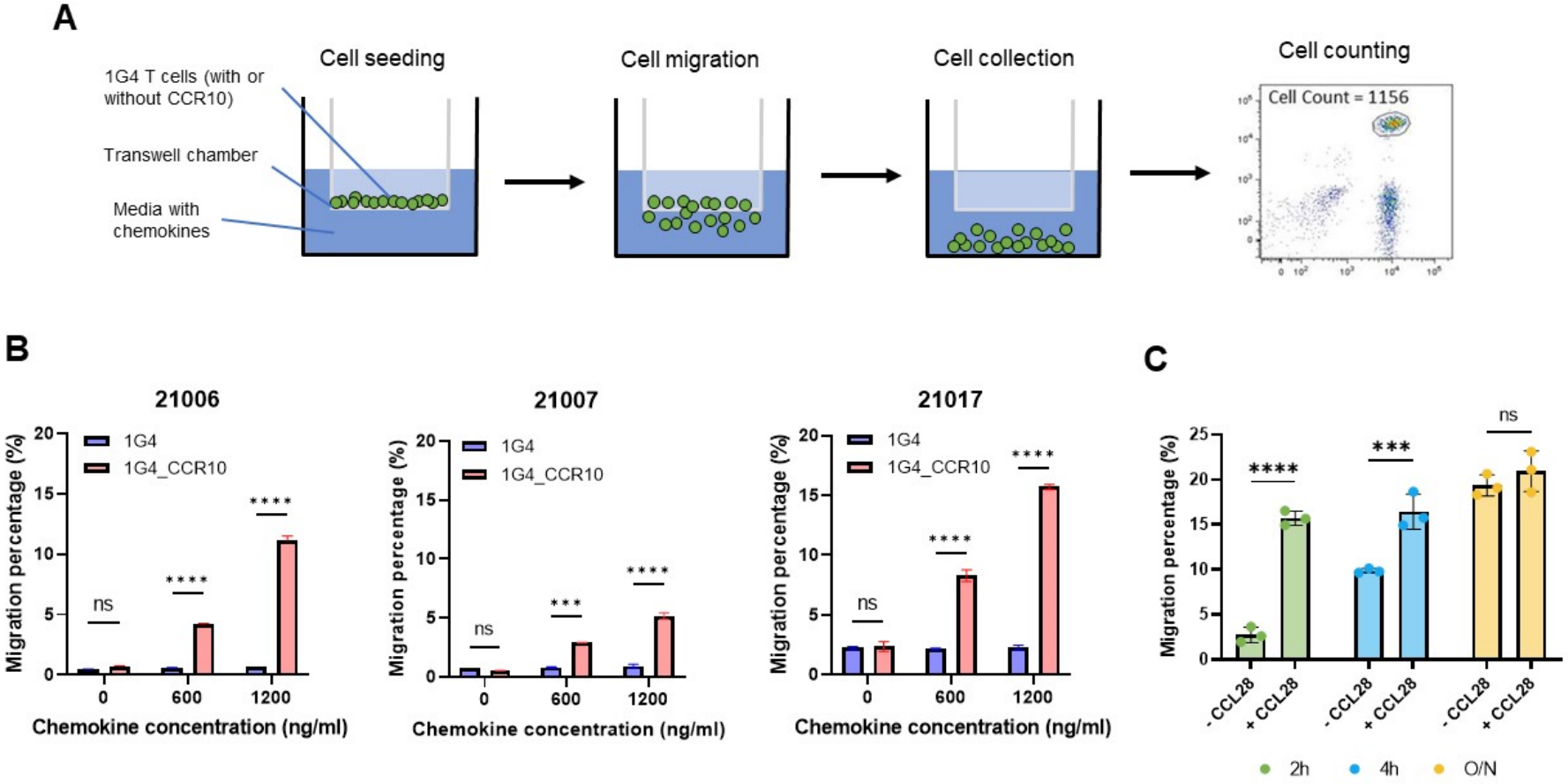
A
Cell seeding
Cell migration
Cell collection
Cell counting
1G4 T cells (with or without CCR10)
Transwell chamber
Media with chemokines
Cell Count = 1156
B
21006
21007
21017
1G4
1G4_CCR10
Migration percentage (%)
Chemokine concentration (ng/ml)
ns
***
****
C
- CCL28
+ CCL28
2h
4h
O/N

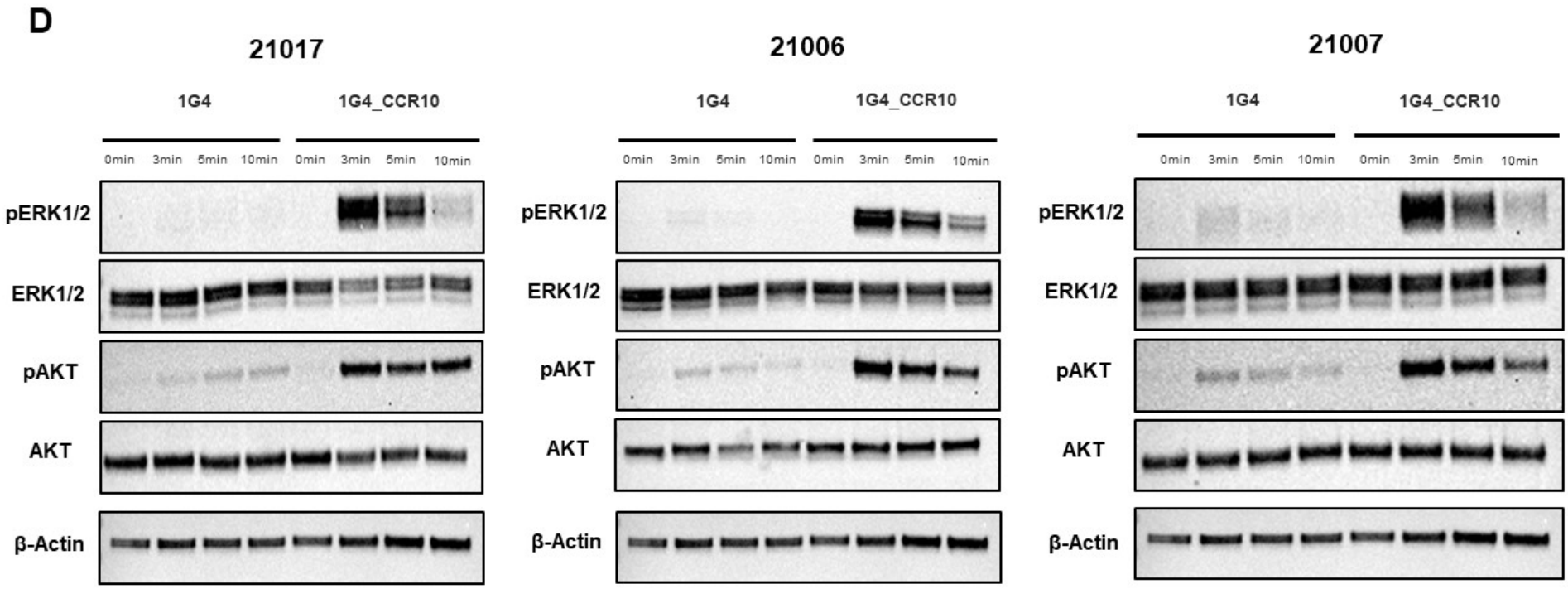
D
21017
1G4
1G4_CCR10
0min 3min 5min 10min 0min 3min 5min 10min
pERK1/2
ERK1/2
pAKT
AKT
β-Actin
21006
1G4
1G4_CCR10
0min 3min 5min 10min 0min 3min 5min 10min
pERK1/2
ERK1/2
pAKT
AKT
β-Actin
21007
1G4
1G4_CCR10
0min 3min 5min 10min 0min 3min 5min 10min
pERK1/2
ERK1/2
pAKT
AKT
β-Actin

Figure 5

CCR10 promotes migration of 1G4 TCR-T *in vitro*. The migration ability of 1G4 TCR-T and CCR10-1G4 dual expressing TCR-T were detected by transwell assay. (A) This figure illustrates a graphical representation of the transwell assay process.(B) Following a 2-hour incubation with varying concentrations of CCL28, or (C) after different time intervals with 1,200 ng/mL of chemokines, the cells that had moved to the lower chamber were assessed through flow cytometry, and the specific migration percentage was calculated using the formula outlined in the Materials and Methods section. (D) To validate migration signaling delivery, chemokine-induced ERK-1/2 and AKT antibodies activation were assessed through Western blotting using phospho-specific anti-ERK-1/2 and phospho-specific anti-AKT. The Western blot was then reprobed with total ERK-1/2 and AKT antibodies to serve as protein loading controls. Additionally, beta-actin, a housekeeping gene, was used as a control. Data represents mean ± SD (n = 3). Two-way ANOVA was conducted for statistical analysis. ***$p < 0.001$, ****$p < 0.0001$.

3-6. CCR10-1G4 dual expressing TCR-T show identical cytotoxic activity as 1G4 TCR-T

To assess the functionality of 1G4 TCR, Jurkat cells were transduced with a vector containing the NFAT-Luciferase gene and a separate vector containing 1G4-CCR10. Subsequently, these cells were co-cultured with NY-ESO-1-pulsed T2 cells to validate the activation response. The degree of Jurkat cell activation increased as the concentration of NY-ESO-1 pulsing increased (Fig. 6A).

1G4 TCR-T and CCR10-1G4 dual-expressing TCR-T were cultured alongside target cells at different effector/target ratios for a period of 24 hours. T cells expressing only 1G4 TCR exhibited higher 1G4 expression levels than T cells co-expressing CCR10-1G4 TCR. To equalize the expression, Mock T cells were mixed with 1G4 TCR-T at a 1:2 ratio, to achieve equivalent 1G4 expression levels. The results revealed no significant difference in tumor-killing ability between the two types of TCR-T (Fig. 6B). Additionally, there was a mild increase in interleukin-2(IL-2) production in CCR10-1G4 dual expressing TCR-T, while interferon-gamma (IFN-γ) production did not change (Fig. 6C). These findings imply that CCR10 expression did not impact the cytotoxicity of TCR-T *in vitro*.

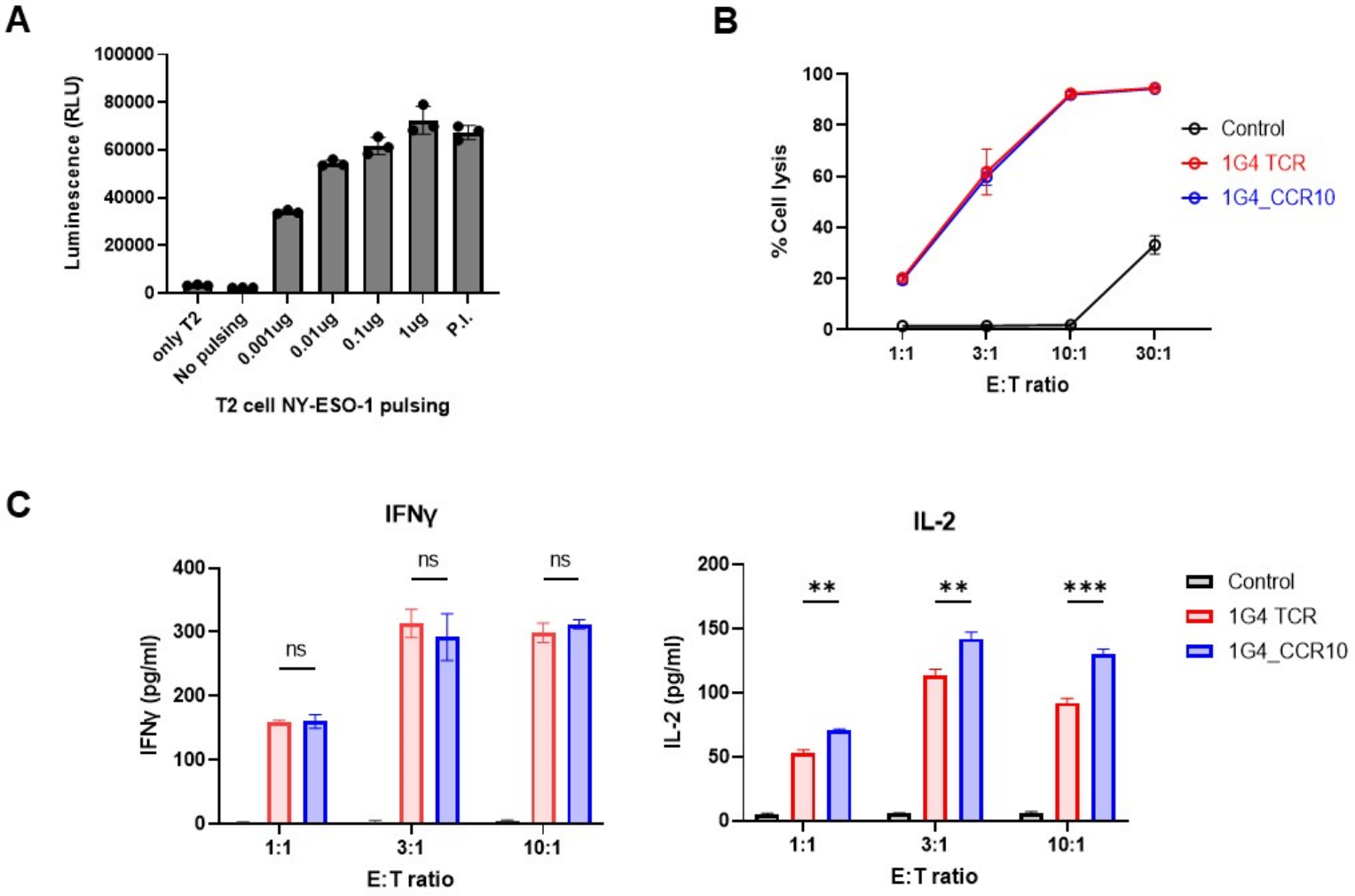
A
Luminescence (RLU)
100000
80000
60000
40000
20000
0
only T2
No pulsing
0.001ug
0.01ug
0.1ug
1ug
P.I.
T2 cell NY-ESO-1 pulsing
B
% Cell lysis
100
80
60
40
20
0
1:1
3:1
10:1
30:1
E:T ratio
Control
1G4 TCR
1G4_CCR10
C
IFNγ
IFNγ (pg/ml)
400
300
200
100
0
ns
ns
ns
1:1
3:1
10:1
E:T ratio
IL-2
IL-2 (pg/ml)
200
150
100
50
0
**
**
***
1:1
3:1
10:1
E:T ratio
Control
1G4 TCR
1G4_CCR10

Figure 6

CCR10-1G4 dual expressing TCR-T showed similar cytotoxicity activity as 1G4 TCR-T. (A) To assess 1G4 TCR activity, Jurkat-NFAT-Luc was employed. After pulsing T2 cells with NY-ESO-1 peptide and β2m, a co-culture was conducted with Jurkat-NFAT-Luc cells for 24 hours. (B, C) Control T, 1G4 TCR-T, or CCR10-1G4 dual expressing TCR-T were co-cultured with A375-Luc/CCL28 cells at E/T ratios of 1:1, 3:1, 10:1 and 30:1 for 24 hours. (B) After co-culture, luciferase measurements were conducted in A375-Luc/CCL28 cells, and the tumor cell death rate was calculated using the formula described in the Materials and Methods section. (C) Cytokine production by T cells co-cultured with A375-Luc/CCL28 cells. Levels of IFN-γ and IL-2 in the supernatant were determined by ELISA. Data represents mean ± SD (n = 3).

3-7. CCR10 Expression Improves the *In Vivo* Anti-Tumor Effect of TCR-T

I explored the possibility of *in vivo* establishment of improved migration of 1G4 TCR-T toward tumor cells by overexpressing CCR10, using xenografts of the human A375-Luc/CCL28 cancer cell line in NOD-SCID mice.

DiR-labeled T cell distribution in mice was imaged at 24 hour intervals over a three-day period. After the initial 24-hour period, DiR fluorescence signals were detected at the tumor site in mice injected with CCR10-1G4 dual-expressing TCR-T. Furthermore, when quantitatively analyzing the intensity of DiR fluorescence signals at the tumor sites after 48 and 72 hours, we observed a roughly 2 fold increase in signal intensity in mice injected with CCR10-1G4 dual-expressing TCR-T compared to those injected with 1G4 TCR-T alone (Fig. 7B). Therefore, upregulating CCR10 in 1G4 TCR-T can boost the movement and penetration of i.v. administered T cells into subcutaneous tumors.

I proceeded to examine whether the heightened tumor migration and infiltration could enhance the *in vivo* cytotoxicity of CCR10-1G4 dual-expressing TCR-T against cancer cells. Tumor loads were similar in all three groups of mice on day 5, 12 and 19. Nonetheless, a slight reduction in tumor burden was noted in mice treated with CCR10-1G4 dual-expressing TCR-T on day 33, while mice treated with 1G4 TCR-T did not show this reduction (Fig. 7C). Therefore, the improved tumor migration and infiltration of CCR10-expressing 1G4 TCR-T may be beneficial in reducing tumor burden *in vivo*.

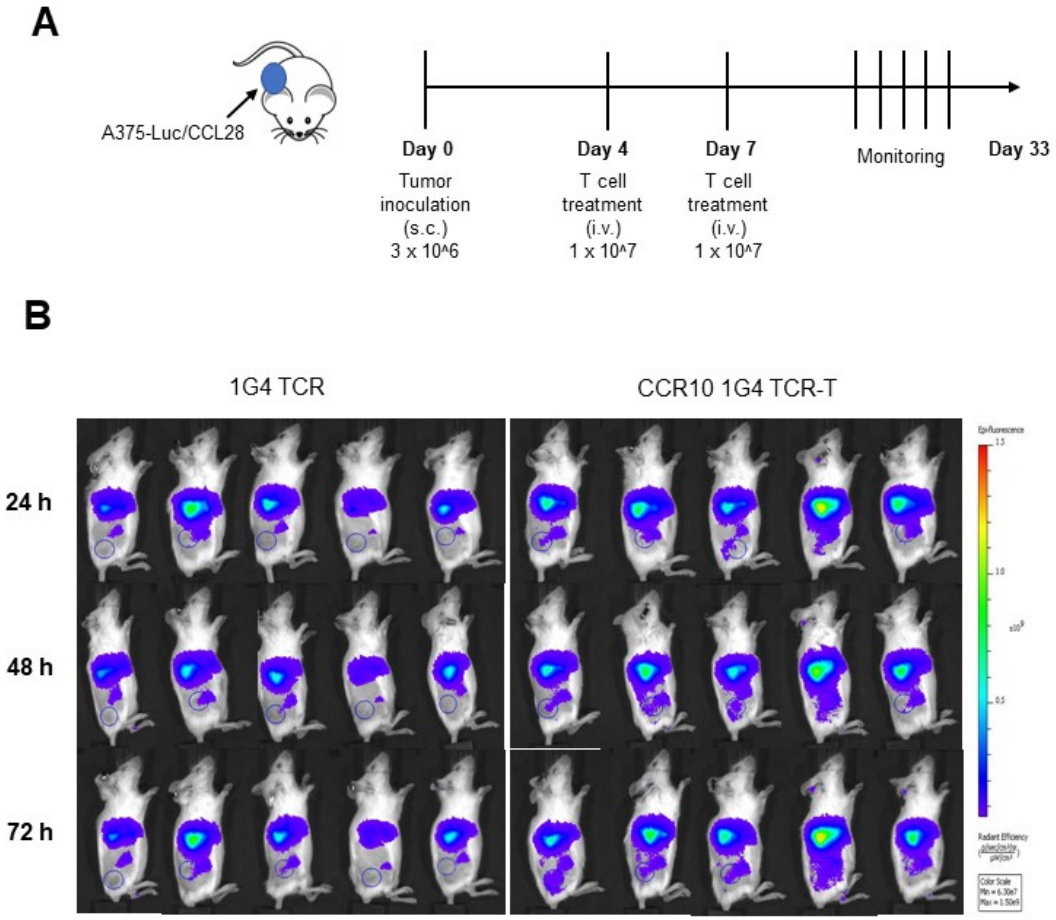
A
A375-Luc/CCL28
Day 0
Tumor inoculation (s.c.) 3 x 10^6
Day 4
T cell treatment (i.v.) 1 x 10^7
Day 7
T cell treatment (i.v.) 1 x 10^7
Monitoring
Day 33
B
1G4 TCR
CCR10 1G4 TCR-T
24 h
48 h
72 h

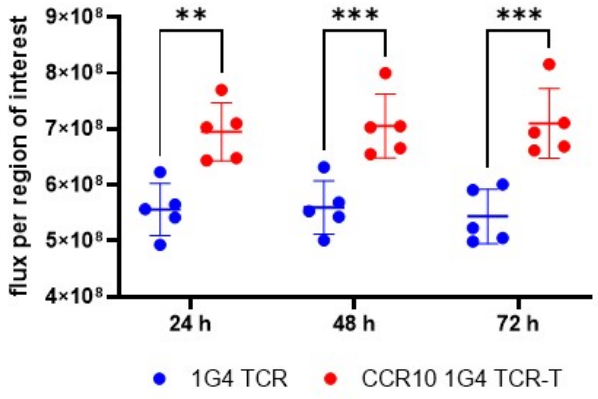
flux per region of interest
9×10⁸
8×10⁸
7×10⁸
6×10⁸
5×10⁸
4×10⁸
**
***
***
24 h
48 h
72 h
1G4 TCR
CCR10 1G4 TCR-T

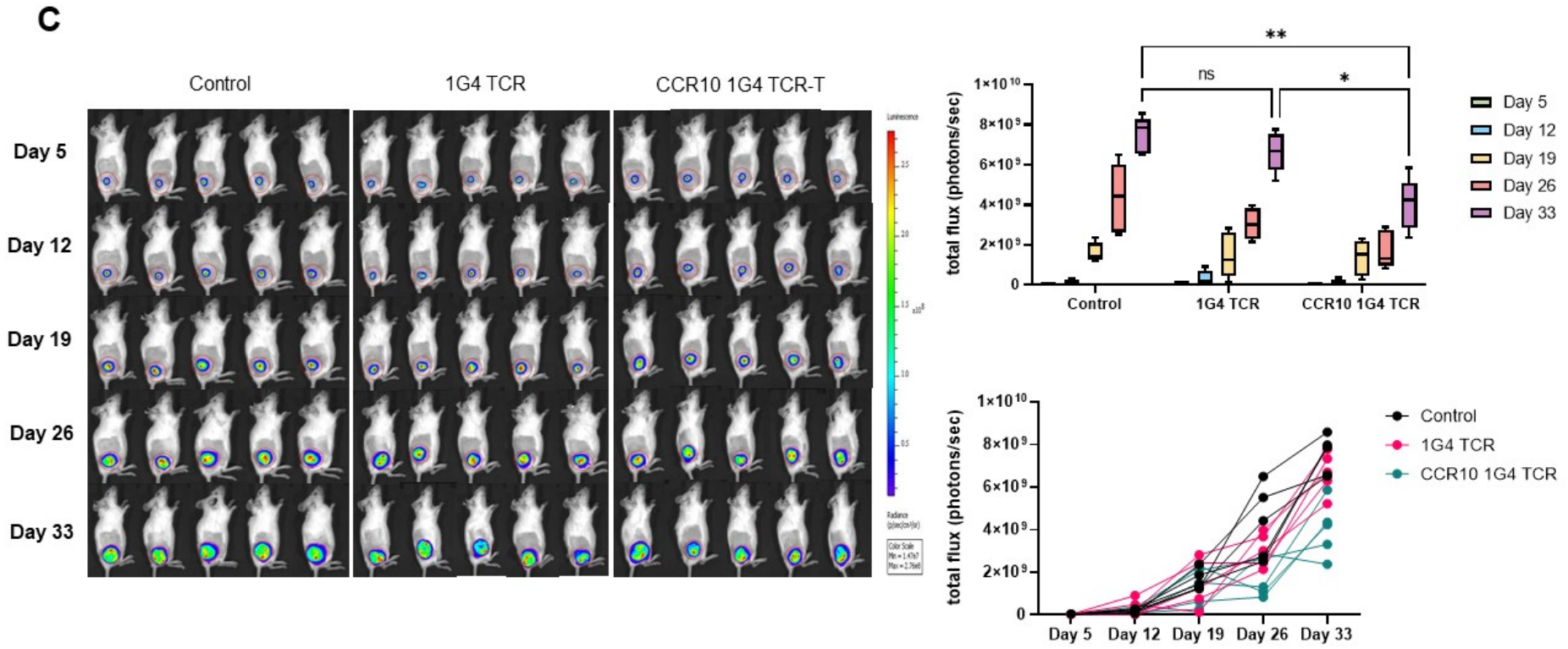
C
Control
1G4 TCR
CCR10 1G4 TCR-T
Day 5
Day 12
Day 19
Day 26
Day 33
**
ns
*
total flux (photons/sec)
1×10¹⁰
8×10⁹
6×10⁹
4×10⁹
2×10⁹
0
Control
1G4 TCR
CCR10 1G4 TCR
Day 5
Day 12
Day 19
Day 26
Day 33
Control
1G4 TCR
CCR10 1G4 TCR
Day 5
Day 12
Day 19
Day 26
Day 33

Figure 7

An animal experiment was conducted to assess the *in vivo* killing efficacy against i.p. xenografts of human A375-Luc/CCL28 cancer cells. (A) Three groups of NOD-SCID mice (n = 5) were administered intraperitoneal (i.p.) injections of A375-Luc/CCL28 cancer cells on day 0. Subsequently, these mice received intravenous injections of PBS, 1G4 TCR-T, or CCR10-1G4 dual-expressing TCR-T. (B) After T cell injection, the mice were subjected to imaging at 24-hour intervals for up to 72 hours. Whole-body imaging of the mice and flux values at the tumor sites, as indicated by blue circles in the images, were presented in the bar graph (n = 5). (C) Tumor bioluminescence imaging was conducted on days 5, 19, 26 and 33 following tumor inoculation. The flux values indicating tumor burden on days 5, 19, 26 and 33 were depicted in a bar graph. Data represents mean ± SD. Two-way ANOVA was conducted for statistical analysis. *$p < 0.05$.

4. Discussion

Table 2. Studies with chemokine receptor engineering

Cell type	Receptor type	Gene overexpression	Target	chemokine receptor	chemokine ligand	Expression	Increase of migration efficiency *in vitro*	Increase of migration efficiency *in vivo*	Tumor volume reduction	Reference
CD3+ T cell	Msln-CAR	Lentivirus	NSCLC	CCR2b, CCR4	CCL2, CCL7, CCL8, CCL12, CCL16	CCR2b: 63% CCR4: 45%	CCR2b: 2.6 times (A549-Mcp 1 9.6 ng/ml/10^6) CCR4: 2.2 times (A549-Mcp 1 9.6 ng/ml/10^6)	N/A	35 days, 100%	(22)
tumor-specific T cells	Pmel-1/Thy1.1+ TCR	Retrovirus	Melanoma	CXCR2	CXCL1, CXCL8	76%	3 times (CXCL1 30 ng/ml) 10 times (B16-CXCL1 35 ng/ml)	2 times	24 days, 70%	(23)
Primary murine and human T cell	CAR-MSLN, CAR-EpCAM	Retrovirus	pancreatic cancer	CCR8	CCL1	76%	7 times (CCL1 10 ng/ml)	N/A	30 days, 60%	(24)
CD3+ T cell	CD70CAR	Lentivirus	GBM, ovarian and pancreatic cancer	CXCR1, CXCR2	CXCL1, CXCL8	CXCR1: 83% CXCR2 : 81%	CXCR1: 9 times (CXCL8 10 ng/ml) CXCR2 : 3.5 times (CXCL8 10 ng/ml)	2 times	18 days, 96%	(25)
CD3+ T cell	EpCAM-CAR, MSLN-CAR	Retrovirus	pancreatic cancer	CXCR6	CXCL16	44%	1.75 times (CXCL16 50 ng/ml)	2.1 times	30 days 100%	(26)
CD3+ T cell	EGFR-CAR	Lentivirus	NSCLC	CXCR5	CXCL13	23%	4h: 2.0 times (CXCL13 5000 ng/ml) 8h: 2.1 times (CXCL13 5000 ng/ml) 16h: 2.3 times (CXCL13 5000 ng/ml)	72h: 2 times 168h: 3 times	25 days 100%	(27)
CD3+ T cell	GPC3-CAR-T	Lentivirus	HCC	CXCR2	CXCL1, CXCL8	32%	9 times (CXCL8 20 ng) 5 times (CXCL8 50 ng) 9.6 times (CXCL8 100 ng) 9 times (CXCL8 200 ng) 7.3 times (CXCL8 500 ng)	N/A	26 days 98%	(28)
NK cell	EGFRvIII-specific CAR	mRNA encoding CXCR1 by electroporation	SCC, ovarian cancer	CXCR1	CXCL1, CXCL8	24h: 90% 48h: 85% 72h: 81%	5 times	10 times	42 days 96%	(29)
Human T cell	GD2-specific CAR	Retrovirus	neuroblastoma	CCR2b	CCL2	CD4+: 41% CD8+: 63%	3 times (CCL2 10 ng/ml)	9.5 times	22 days 98%	(30)
Primary T cell	EGFR-CAR	Lentivirus	NSCLC	CCR6	CCL20	23%	4.5 times (A549-CCL20 0.9 ng/ml)	2.5 times	21 days 99%	(31)
TIL	N/A	RNA electroporation	malignant melanoma	CXCR1	CXCL1, CXCL8	40%	3.3 times	N/A	N/A	(32)
CD8+ T cell	HLA-A*2402-restricted and WT1235–243 nonapeptide-specific TCR	Retrovirus	Lung Cancer	CCR2	CCL2	90%	4.1 times	2.6 times	21 days, 50%	(33)

*NSCLC: Non-Small Cell Lung Cancer / *HL: Relapsed, refractory CD30+ Hodgkin / *CTCL: Cutaneous T cell Lymphoma / *GBM: Glioblastoma / *HCC: Hepatocellular carcinoma / *SCC: Squamous cell carcinoma / *PBMCs: Peripheral blood mononuclear cells / *ATLs: Autologous activated T lymphocytes / *Msln-CAR: CAR specific for tumor antigen mesothelin / *N/A: not applicable.

Chemokine receptor engineering clinical trial.

Immune Cell type	Receptor type	Target	chemokine receptor	chemokine ligand	number	Status	phase
TILs	CAR (NGFR)	Melanoma	CXCR2	CXCL1, CXCL8	NCT01740557	Active, not recruiting	1/2 phase
ATLs	CAR (CD30 specific CAR)	HL and CTCL	CCR4	CCL22, CCL17	NCT03602157	Recruiting	1 phase
Autologous T cell	CAR (EGFR)	NSCLC	CXCR5	CXCL13	NCT05060796	Recruiting	Early phase 1

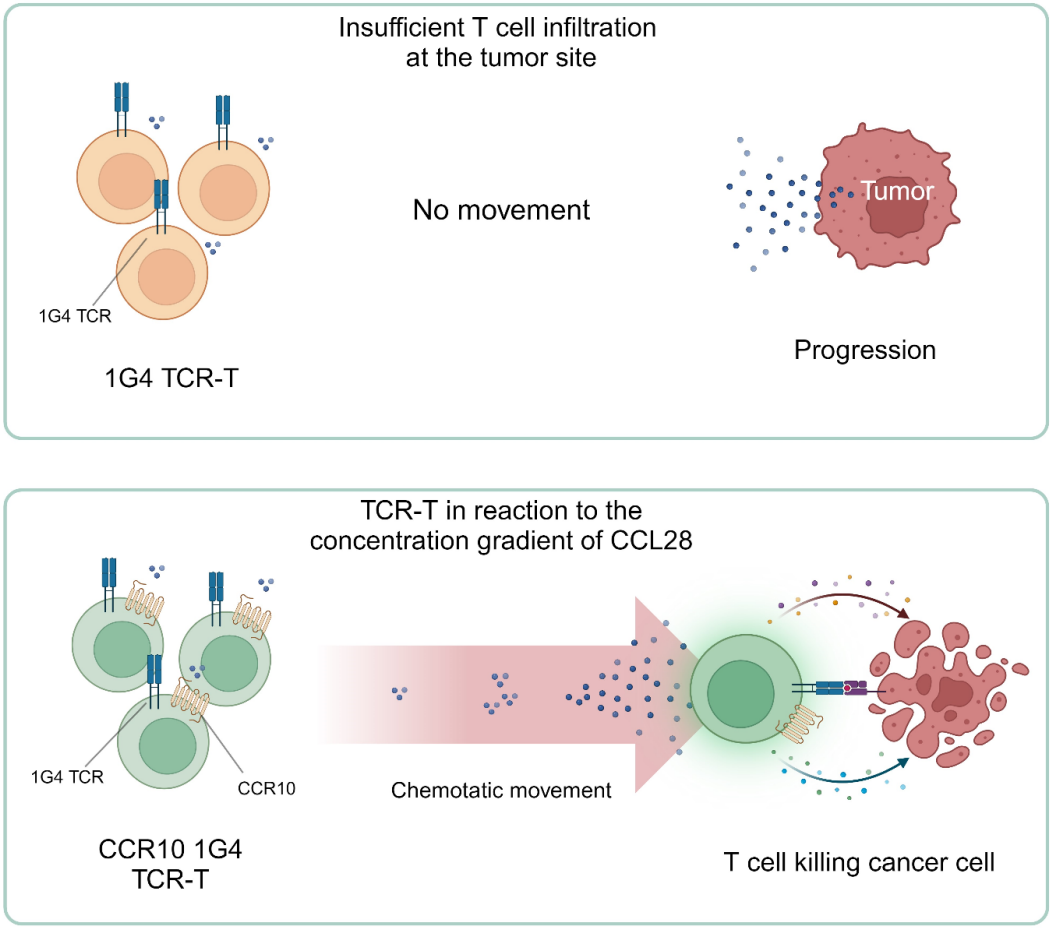

(Created in BioRender.com)

Previous studies have observed an increase in immune cell trafficking using chemokine receptors (Table 2). Based on this, we hypothesized that attaching chemokine receptors that match the chemokine ligands present in the tumor microenvironment to T cells could enhance their capacity to migrate and infiltrate the tumor microenvironment. In this study, I have demonstrated that engineered T cells co-express the TCR directed toward tumor-associated antigen NY-ESO-1 (1G4) and CCR10, which has not been fully explored for ACT previously, lead to a more rapid migration to A375 melanoma cells compared to TCR-expressing T cells lacking CCR10. Furthermore, CCR10-1G4 dual expressing TCR-T can treat melanoma *in vitro* and *in vivo*.

The TCR-T technique utilizing 1G4 TCR has been widely recognized and effectively employed in humans (34). Therefore, I employed A375 melanoma cells, which are commonly used in 1G4 TCR-T studies, to reliably analyze the impact of adding CCR10 without being affected by the degradation of killing ability. Additionally, considering that the most frequent HLA type in Koreans is HLA-A*02, found in approximately 26.4% of the total population, the choice of the A375 cell line was particularly appropriate for our research (35).

CCR10, which is a shared receptor for CCL27 and CCL28, has been reported to be expressed only in specific cell types, such as T-regulatory cells, memory CD4+ T cells, Th 22 cells, and plasmacytoid dendritic cells (36, 37). On the other hand, CCR10 was found to express at low levels in CD8+ T cells commonly used in cell-based therapies (38, 39). My study further proves that CCR10 is not expressed in activated human T cells. Because CCL28 is significantly increased in solid cancers including breast cancer and lung cancer, the lack of CCR10 may hinder trafficking of T cells within these tumors. Therefore, CCR10 could be an ideal candidate to

improve T cell trafficking.

One significant obstacle in the optimization of T cell trafficking based on chemokine receptors is determining whether tumor-secreted chemokines are adequate for recruiting modified T cells. In previous studies, NK cells were treated with Glatiramer Acetate(GA), Dimethyl Fumarate(DMF), and Monomethyl Fumarate(MMF) to increase the efficiency of NK cell migration to targets by inducing the overexpression of CCR10 (40). However, in this experiment, the expression of CCR10 in NK cells showed only 8% expression when preincubated overnight with 100 uM of GA or DMF. To address this efficiency issue, I adopted a different approach by overexpressing CCR10 in T cells using a viral vector. This marks the first instance of CCR10 overexpression achieved through genetic engineering.

I evaluated the simultaneous overexpression of 1G4 TCR and CCR10, achieving an expression efficiency of 25%. Drawing from previous studies that analyzed gene expression downstream of the promoter, considering linker type, arrangement order, and combination methods, I observed a trend of decreasing efficiency in the order of P2A, T2A, and E2A linkers. Furthermore, a combination of different linkers, specifically P2A and T2A, was more effective than using the same linker, P2A (41). Based on these findings, the P2A linker was inserted between TCR alpha and beta, and the T2A linker was placed between TCR and CCR10 to enhance the expression efficiency.

In a prior study, co-expression of CXCR1 and NKG2D CAR in NK cells was achieved using mRNA electroporation, resulting in a remarkable increase in expression levels to 95%. However, this elevated expression was observed to be transient, lasting only for 72 hours (29). mRNA electrophoresis has a unique advantage in being easy to use and highly reproducible. However, it has the

disadvantage of short-term expression, making it effective primarily for short-lived cells. To overcome this limitation, viral transduction was employed. This approach enables long-term expression and ensures functional persistence of cells expressing the chemokine receptor. In migration test using the transwell migration plate, I observed that at 25% CCR10 receptor expression, the chemotaxis index (the movement of a living thing or object in response to a chemical stimulus) was approximately 3.8 times higher when exposed to a concentration of 600 ng of human recombinant CCL28, and it was 4.4 times higher at a concentration of 1,200 ng. In previous studies, it was observed that EGFR-CAR-CXCR5 exhibited a 23% expression of CXCR5 and a 2.3-fold increase in the chemotaxis index at a CXCL13 concentration of 5,000 ng/ml compared to the control (27). Similarly, EpCAM-CAR-CXCR6 showed a 44% expression of CXCR6, and the chemotaxis index increased 1.75 times at a CXCL16 concentration of 50 ng/ml (26). While my study achieved favorable results with higher expression levels compared to previous studies, it's important to recognize that differences in experimental conditions exist between studies. Moreover, because the expression of chemokine ligands can vary among individual patients, this diversity further complicates the comparative analysis in clinical trial settings. Therefore, a comprehensive assessment is essential for a full understanding of the significance of my research findings.

To further validate the effect of CCR10 in T cell trafficking *in vivo*, I also employed the newly established A375-Luc/CCL28 CDX tumor model, which allowed us to monitor the trafficking of transferred tumor specific CCR10 T cells *in vivo*. I found that tumor-specific T cell trafficking to tumor sites was improved following CCR10 transduction of the T cells. Both in vitro and *in vivo* experiments have supported the initial hypothesis that overexpressing CCR10 enhances the migration

of TCR-T to tumor sites positive for CCL28. Although the *in vivo* anti-tumor effects exhibited modest outcomes, I highlight the significance of the early substantial increase in T cell migration. Recognizing that effective T cell migration to the target tumor is imperative for the manifestation of anti-tumor effects, I assert that this enhanced migration is equally pivotal alongside the reduction in tumor size. Moreover, there are side effects associated with sudden immune reactions, such as cytokine release syndrome, which is one of the challenges in ACT. However, the manifestation of anti-tumor effects from day 33 onwards could potentially have a positive impact on mitigating these issues.

The availability of chemokine ligands specifically binding to the CCR10 receptor is limited. In cases where tumor cells do not express CCL28, the effectiveness of T cell trafficking enhancement may be compromised. Identifying alternative chemokine receptors with broader ligand specificities is a valuable avenue for improving the versatility of ACT strategies. While my study used *in vivo* models to validate enhanced T cell trafficking, it's important to note that these models may not completely replicate the intricacies of human tumors. Differences between murine models and human patients, along with unique aspects of the tumor microenvironment, need to be considered when applying our results in a clinical context. Lastly, the sustainability of the effect we observed following CCR10 transduction remains uncertain. Conducting studies with extended duration to evaluate how enduring and effective CCR10-modified T cells are in real clinical scenarios will be crucial for determining the practicality of this therapeutic approach.

In conclusion, my study has illuminated the potential of CCR10 in enhancing T cell trafficking to tumor sites, offering a promising avenue for improving ACT in the context of solid tumors.

5. Reference

1. Rohaan MW, Wilgenhof S, Haanen JBAG (2019) Adoptive cellular therapies: the current landscape. Virchows Arch. 474: 449-61. doi: 10.1007/s00428-018-2484-0

2. Holstein SA, Lunning MA (2020) CAR T-Cell Therapy in Hematologic Malignancies: A Voyage in Progress. Clin Pharmacol Ther. 107: 112-22. doi:10.1002/cpt.1674

3. Zhao LJ, Cao YJ (2019) Engineered T Cell Therapy for Cancer in the Clinic. Front Immunol. 10. doi: ARTN 225010.3389/fimmu.2019.02250

4. Sterner RC, Sterner RM (2021) CAR-T cell therapy: current limitations and potential strategies. Blood Cancer J. 11. doi: ARTN 6910.1038/s41408-021-00459-7

5. Yeku O, Li X, Brentjens RJ (2017) Adoptive T-Cell Therapy for Solid Tumors. Am Soc Clin Oncol Educ Book. 37: 193-204. doi: 10.1200/EDBK_180328

6. Dagar G, Gupta A, Masoodi T et al. (2023) Harnessing the potential of CAR-T cell therapy: progress, challenges, and future directions in hematological and solid tumor treatments. J Transl Med. 21. doi: ARTN 44910.1186/s12967-023-04292-3

7. Morotti M, Albukhari A, Alsaadi A et al. (2021) Promises and challenges of adoptive T-cell therapies for solid tumours. Brit J Cancer. 124: 1759-76. doi: 10.1038/s41416-021-01353-6

8. Akbay EA, Koyama S, Liu Y et al. (2017) Interleukin-17A Promotes Lung Tumor Progression through Neutrophil Attraction to Tumor Sites and Mediating

Resistance to PD-1 Blockade. J Thorac Oncol. 12: 1268-79. doi: 10.1016/j.jtho.2017.04.017

9. Bauer CA, Kim EY, Marangoni F, Carrizosa E, Claudio NM, Mempel TR (2014) Dynamic Treg interactions with intratumoral APCs promote local CTL dysfunction. J Clin Invest. 124: 2425-40. doi: 10.1172/Jci66375

10. Linke B, Dos Santos SM, Picard-Willems B, Keese M, Harder S, Geisslinger G, Scholich K (2019) CXCL16/CXCR6-mediated adhesion of human peripheral blood mononuclear cells to inflamed endothelium. Cytokine. 122. doi: ARTN 15408110.1016/j.cyto.2017.06.008

11. Griffith JW, Sokol CL, Luster AD (2014) Chemokines and Chemokine Receptors: Positioning Cells for Host Defense and Immunity. Annu Rev Immunol. 32: 659-702. doi: 10.1146/annurev-immunol-032713-120145

12. Curiel TJ, Coukos G, Zou LH et al. (2004) Specific recruitment of regulatory T cells in ovarian carcinoma fosters immune privilege and predicts reduced survival. Nat Med. 10: 942-9. doi: 10.1038/nm1093

13. Lim WA, June CH (2017) The Principles of Engineering Immune Cells to Treat Cancer. Cell. 168: 724-40. doi: 10.1016/j.cell.2017.01.016

14. Lee HJ, Kim YA, Sim CK et al. (2017) Expansion of tumor-infiltrating lymphocytes and their potential for application as adoptive cell transfer therapy in human breast cancer. Oncotarget. 8: 113345-59. doi: 10.18632/oncotarget.23007

15. Poschke I, Faryna M, Bergmann F et al. (2016) Identification of a tumor-reactive T-cell repertoire in the immune infiltrate of patients with resectable

pancreatic ductal adenocarcinoma. Oncoimmunology. 5. doi: ARTN e124085910.1080/2162402X.2016.1240859

16. Bolger AM, Lohse M, Usadel B (2014) Trimmomatic: a flexible trimmer for Illumina sequence data. Bioinformatics. 30: 2114-20. doi: 10.1093/bioinformatics/btu170

17. Dobin A, Gingeras TR (2016) Optimizing RNA-Seq Mapping with STAR. Methods Mol Biol. 1415: 245-62. doi: 10.1007/978-1-4939-3572-7_13

18. Li B, Dewey CN (2011) RSEM: accurate transcript quantification from RNA-Seq data with or without a reference genome. Bmc Bioinformatics. 12. doi: Artn 32310.1186/1471-2105-12-323

19. Love MI, Huber W, Anders S (2014) Moderated estimation of fold change and dispersion for RNA-seq data with DESeq2. Genome Biol. 15. doi: ARTN 55010.1186/s13059-014-0550-8

20. Lim HD, Lane JR, Canals M, Stone MJ (2021) Systematic Assessment of Chemokine Signaling at Chemokine Receptors CCR4, CCR7 and CCR10. Int J Mol Sci. 22. doi: ARTN 423210.3390/ijms22084232

21. Wargo JA, Robbins PF, Li Y et al. (2009) Recognition of NY-ESO-1+tumor cells by engineered lymphocytes is enhanced by improved vector design and epigenetic modulation of tumor antigen expression. Cancer Immunol Immun. 58: 383-94. doi: 10.1007/s00262-008-0562-x

22. Wang Y, Wang J, Yang X et al. (2021) Chemokine Receptor CCR2b Enhanced Anti-tumor Function of Chimeric Antigen Receptor T Cells Targeting Mesothelin in a

Non-small-cell Lung Carcinoma Model. Front Immunol. 12: 628906. doi: 10.3389/fimmu.2021.628906

23. Peng W, Ye Y, Rabinovich BA et al. (2010) Transduction of tumor-specific T cells with CXCR2 chemokine receptor improves migration to tumor and antitumor immune responses. Clin Cancer Res. 16: 5458-68. doi: 10.1158/1078-0432.CCR-10-0712

24. Cadilha BL, Benmebarek MR, Dorman K et al. (2021) Combined tumor-directed recruitment and protection from immune suppression enable CAR T cell efficacy in solid tumors. Sci Adv. 7. doi: 10.1126/sciadv.abi5781

25. Jin L, Tao H, Karachi A et al. (2019) CXCR1- or CXCR2-modified CAR T cells co-opt IL-8 for maximal antitumor efficacy in solid tumors. Nat Commun. 10: 4016. doi: 10.1038/s41467-019-11869-4

26. Lesch S, Blumenberg V, Stoiber S et al. (2021) T cells armed with C-X-C chemokine receptor type 6 enhance adoptive cell therapy for pancreatic tumours. Nat Biomed Eng. 5: 1246-60. doi: 10.1038/s41551-021-00737-6

27. Li GC, Guo JT, Zheng YF, Ding W, Han ZP, Qin LY, Mo WJ, Luo M (2021) CXCR5 guides migration and tumor eradication of anti-EGFR chimeric antigen receptor T cells. Mol Ther-Oncolytics. 22: 507-17. doi: 10.1016/j.omto.2021.07.003

28. Liu G, Rui W, Zheng H, Huang D, Yu F, Zhang Y, Dong J, Zhao X, Lin X (2020) CXCR2-modified CAR-T cells have enhanced trafficking ability that improves treatment of hepatocellular carcinoma. Eur J Immunol. 50: 712-24. doi: 10.1002/eji.201948457

29. Ng YY, Tay JCK, Wang S (2020) CXCR1 Expression to Improve Anti-Cancer Efficacy of Intravenously Injected CAR-NK Cells in Mice with Peritoneal Xenografts. Mol Ther Oncolytics. 16: 75-85. doi: 10.1016/j.omto.2019.12.006

30. Craddock JA, Lu A, Bear A, Pule M, Brenner MK, Rooney CM, Foster AE (2010) Enhanced Tumor Trafficking of GD2 Chimeric Antigen Receptor T Cells by Expression of the Chemokine Receptor CCR2b. J Immunother. 33: 780-8. doi: 10.1097/CJI.0b013e3181ee6675

31. Jin LY, Cao L, Zhu YJ, Cao JN, Li XY, Zhou JX, Liu B, Zhao TB (2021) Enhance anti-lung tumor efficacy of chimeric antigen receptor-T cells by ectopic expression of C?C motif chemokine receptor 6. Sci Bull. 66: 803-12. doi: 10.1016/j.scib.2020.12.027

32. Sapoznik S, Ortenberg R, Galore-Haskel G et al. (2012) CXCR1 as a novel target for directing reactive T cells toward melanoma: implications for adoptive cell transfer immunotherapy. Cancer Immunol Immunother. 61: 1833-47. doi: 10.1007/s00262-012-1245-1

33. Asai H, Fujiwara H, An J et al. (2013) Co-introduced functional CCR2 potentiates in vivo anti-lung cancer functionality mediated by T cells double gene-modified to express WT1-specific T-cell receptor. Plos One. 8: e56820. doi: 10.1371/journal.pone.0056820

34. Rapoport AP, Stadtmauer EA, Binder-Scholl GK et al. (2015) NY-ESO-1-specific TCR-engineered T cells mediate sustained antigen-specific antitumor effects in myeloma. Nat Med. 21: 914-21. doi: 10.1038/nm.3910

35. Park HJ, Kim YJ, Kim DH, Kim J, Park KH, Park JW, Lee JH (2016) HLA Allele

Frequencies in 5802 Koreans: Varied Allele Types Associated with SJS/TEN According to Culprit Drugs. Yonsei Med J. 57: 118-26. doi: 10.3349/ymj.2016.57.1.118

36. Strazza M, Mor A (2017) Consider the Chemokines: a Review of the Interplay Between Chemokines and T Cell Subset Function. Discov Med. 24: 31-9.

37. (n.d.) The Human Protein Atals. https://www.proteinatlas.org/ENSG00000184451-CCR10. Accessed July 19, 2023

38. Fyhrquist N, Wolff H, Lauerma A, Alenius H (2012) CD8+T Cell Migration to the Skin Requires CD4+Help in a Murine Model of Contact Hypersensitivity. Plos One. 7. doi: ARTN e4103810.1371/journal.pone.0041038

39. Hudak S, Hagen M, Liu Y, Catron D, Oldham E, McEvoy LM, Bowman EP (2002) Immune surveillance and effector functions of CCR10(+) skin homing T cells. J Immunol. 169: 1189-96. doi: DOI 10.4049/jimmunol.169.3.1189

40. Maghazachi AA, Sand KL, Al-Jaderi Z (2016) Glatiramer Acetate, Dimethyl Fumarate, and Monomethyl Fumarate Upregulate the Expression of CCR10 on the Surface of Natural Killer Cells and Enhance Their Chemotaxis and Cytotoxicity. Front Immunol. 7. doi: ARTN 43710.3389/fimmu.2016.00437

41. Liu ZQ, Chen O, Wall JBJ, Zheng M, Zhou Y, Wang L, Vaseghi HR, Qian L, Liu JD (2017) Systematic comparison of 2A peptides for cloning multi-genes in a polycistronic vector. Sci Rep-Uk. 7. doi: ARTN 219310.1038/s41598-017-02460-2

6. Abstract (in Korea)

고형 종양에 대한 Adoptive T 세포 치료의 효과는 종양 부위로의 T 세포 이동이 부족하다는 이유로 여전히 최적화되지 않았습니다. 이에 따라, 한 가지 유망한 전략은 T 세포를 해당 부위로 유도하기 위해 tumor-specific chemokine을 활용하는 것입니다. 이러한 유도는 T 세포 내에서 해당 chemokine에 대응하는 chemokine 수용체가 발현된다는 가정하에 이루어집니다. TCGA와 GTEx의 RNA-seq 데이터 분석을 통해, 유방암과 폐암에서 chemokine CCL28의 높은 발현을 확인하였습니다. 그러나, CCL28의 수용체인 CCR10은 인간 말초 T 세포, 종양 침윤 T 세포, 그리고 활성화된 CAR-T 세포 모두에서 부족하게 발현되었습니다. 따라서 연구의 목표는 CCR10의 유도 잠재력을 활용하여 T 세포를 종양 부위로 유도하고 종양 면역 치료의 효과를 향상시키는 것이었습니다. 종양에 효과를 보이기 위해 클로닝과 lenti virus를 이용하여 1G4 TCR을 T 세포에 발현시킨 후, CCR10을 공동 발현시켰습니다. CCR10-1G4 공동 발현 TCR-T는 시험관 내 (*in vitro*)에서 1G4 TCR-T 세포와 동일한 세포 독성을 보이지만, 이동 능력이 증가 하는 것을 확인하였습니다. 암세포 유래 이종 이식 종양 모델 (CDX) 에서 CCR10-1G4 공동발현 TCR-T 세포를 투여한 실험군에서, 종양 부위로의 생체 내 이동이 1G4 TCR-T 에 비해 증가하는 것을 확인하였습니다. 또한, CCR10-1G4 공동발현 TCR-T를 주입한 실험군의 종양 부담이 약간 감소한 것을 관찰하였습니다. 이 연구는 T 세포의 유도 능력을 증가시키는 것뿐만 아니라 악성 종양을 대상으로 하는 새로운 치료법 개발 가능성을 제시합니다.

Supplemental information

Table 1. BRC

Rate	Gene	TCGA_tumor_breast	GTEx_breast	ABS(log2FC)	Rate	Gene	TCGA_tumor_breast	GTEx_breast	ABS(log2FC)
1	CCL3L1	4.38359022	#N/A	#N/A	30	CXCL17	5.600659417	-0.900517066	6.501176484
2	CXCL12	10.85647093	-5.715566847	16.57203778	31	CXCL1	2.612683267	-3.73833653	6.351019797
3	CCL4	6.428255211	-8.122488824	14.55074404	32	CCL15	-5.155263245	0.820502604	5.975765849
4	CMTM4	10.27016993	-3.613869374	13.8840393	33	CMTM1	6.657413782	0.760399227	5.897014555
5	CCL14-CCL15	-8.91430427	4.959562477	13.87386675	34	CCL11	3.713157346	-1.84737596	5.560533306
6	CCL5	9.004945451	-4.542872686	13.54781814	35	CXCL9	9.498072359	4.025609745	5.472462614
7	CXCL14	10.68841867	-2.664870766	13.35328944	36	CCL24	-7.290682783	-2.529626141	4.761056642
8	CMTM7	8.324772323	-4.943604421	13.26837674	37	CXCL10	8.779746222	4.040581464	4.739164758
9	CX3CL1	9.640510241	-3.575170482	13.21568072	38	CCL2	8.424248799	3.977284029	4.44696477
10	CKLF	8.427833921	-4.15127297	12.57910689	39	XCL2	2.374305548	-2.049370469	4.423676018
11	TNFSF10	11.47044045	-0.32633943	11.79677988	40	CCL7	-1.240912767	-5.254506342	4.013593574
12	CXCL16	10.26084207	-1.360361781	11.62120385	41	PF4	-8.109688135	-4.216010067	3.893678068
13	CCL20	2.339478358	-9.035753403	11.37523176	42	CMTM2	0.013599417	3.621819038	3.608219621

14	CMTM3	10.14948488	-0.926617659	11.07610254	43	CCL8	5.415192467	2.428555568	2.986636899
15	CCL14	6.811878338	-4.100314334	10.91219267	44	CMTM5	-3.653318304	-6.610848015	2.957529711
16	CCL3	6.492531369	-3.56667404	10.05920541	45	CXCL13	6.843544263	4.08030562	2.763238643
17	CCL28	6.166089118	-3.665839288	9.831928406	46	CXCL11	6.898529665	4.163412825	2.735116839
18	PF4V1	-7.17035921	1.880025393	9.050384603	47	CCL25	-2.665481387	-0.01262975	2.652851637
19	CMTM6	11.40635952	2.807876837	8.598482678	48	CCL4L2	5.911865795	3.37992712	2.531938674
20	CXCL2	3.745196173	-4.770167015	8.515363188	49	IL8	5.19688616	3.002404937	2.194481224
21	CCL18	5.223266156	-2.777667311	8.000933467	50	CXCL6	-1.289895815	0.744596597	2.034492412
22	CCL19	6.455706491	-1.459234274	7.914940765	51	CCL13	2.918834145	1.023627017	1.895207128
23	CMTM8	7.33120967	-0.398780974	7.729990644	52	CCL16	-3.706708812	-1.918371797	1.788337015
24	CCL1	-6.88963423	-0.041423524	6.848210706	53	CCL23	-0.556832778	1.218327894	1.775160672
25	XCL1	2.301235756	-4.446524491	6.747760247	54	CXCL3	0.168633607	-1.418062864	1.586696471
26	CCL27	-6.237281576	0.507577572	6.744859148	55	CCL21	5.576094247	4.08396985	1.492124396
27	CCL17	2.265056638	-4.472945605	6.738002242	56	CCL3L3	-0.912217567	-2.285121681	1.372904113
28	PPBP	-5.967062083	0.720171629	6.687233712	57	CXCL5	0.745635557	1.925229005	1.179593447
29	CCL22	6.465869715	-0.123099948	6.588969663	58	CCL26	1.03932431	0.240631748	0.798692562

Table 2. LUSC

Rate	Gene	TCGA_tumor_LUSC	GTEx_Lung	ABS(log2FC)	Rate	Gene	TCGA_tumor_LUSC	GTEx_breast	ABS(log2FC)
1	CCL3L1	4.282195882	#N/A	#N/A	30	CXCL3	5.481413965	-1.414918468	6.896332434
2	CCL20	7.646763503	-9.0371137	16.6838772	31	CCL22	6.743547018	-0.121789179	6.865336197
3	CCL4	7.332378678	-8.121418378	15.45379706	32	CCL27	-5.281951952	0.507800707	5.789752658
4	CXCL12	9.003700676	-5.711969811	14.71567049	33	CXCL6	6.502016304	0.745779656	5.756236648
5	CX3CL1	10.8956753	-3.576200488	14.47187579	34	XCL2	3.609218877	-2.043174528	5.652393404
6	CCL5	9.569892837	-4.542921912	14.11281475	35	CCL1	-5.683555227	-0.041512569	5.642042658
7	CMTM7	8.776737635	-4.942406426	13.71914406	36	CMTM1	6.378926831	0.760416707	5.618510124
8	CMTM4	9.850049113	-3.612567138	13.46261625	37	CXCL9	9.617412163	4.028131114	5.589281049
9	CXCL1	9.127981718	-3.737580465	12.86556218	38	CCL2	9.285741632	3.977682136	5.308059496
10	CCL18	10.07951216	-2.776079784	12.85559195	39	CCL13	5.911179522	1.022871161	4.888308361
11	CXCL14	9.992735676	-2.66201104	12.65474672	40	CCL21	8.955825258	4.084048528	4.87177673
12	CKLF	8.276668911	-4.143342964	12.42001188	41	CXCL10	8.833289645	4.040236923	4.793052722
13	TNFSF10	12.03099624	-0.325995977	12.35699222	42	CXCL13	8.298909164	4.080283216	4.218625948
14	CXCL2	7.484290287	-4.767556664	12.25184695	43	CXCL5	6.038144681	1.924147079	4.113997603
15	CXCL16	10.67543785	-1.360862383	12.03630023	44	CMTM5	-2.65093441	-6.612594409	3.961659999

16	CCL14-CCL15	-6.406498365	4.959097597	11.36559596	45	PF4V1	-1.80484794	1.881651574	3.686499515
17	CCL3	7.145695174	-3.563608469	10.70930364	46	CCL26	3.887893909	0.241288922	3.646604987
18	CXCL17	9.585969215	-0.900788883	10.4867581	47	CCL16	-5.138053465	-1.914747655	3.223305811
19	CMTM3	9.548350661	-0.925042308	10.47339297	48	CCL4L2	6.34585423	3.381056908	2.964797323
20	CCL14	5.886167974	-4.098422478	9.984590451	49	CCL8	5.304496759	2.428328724	2.876168035
21	XCL1	4.973372867	-4.442123275	9.415496142	50	CCL15	-2.043031051	0.821471173	2.864502224
22	CCL28	5.297081177	-3.664398663	8.96147984	51	CCL24	0.295145369	-2.523984539	2.819129908
23	CCL19	7.364391052	-1.456895438	8.821286489	52	CMTM2	1.463513251	3.623041524	2.159528274
24	CMTM6	11.36508114	2.807684539	8.557396602	53	CXCL11	6.192614701	4.162994911	2.02961979
25	CCL17	3.377749664	-4.472438144	7.850187808	54	PF4	-2.582044478	-4.216090348	1.63404587
26	CCL7	2.255232631	-5.250982663	7.506215294	55	CCL25	-1.31851217	-0.01318684	1.30532533
27	CMTM8	7.055719436	-0.398715859	7.454435295	56	PPBP	-0.28297395	0.72335953	1.006333479
28	CCL11	5.254972522	-1.846978396	7.101950918	57	CCL23	1.860433162	1.217797751	0.642635412
29	IL8	10.07516799	3.003951137	7.07121685	58	CCL3L3	-1.53525039	-2.281441678	0.746191289

Table 3. LUAD

Rate	Gene	TCGA_tumor_LUAD	GTEx_breast	ABS(log2FC)	Rate	Gene	TCGA_tumor_LUAD	GTEx_breast	ABS(log2FC)
1	CCL3L1	4.129906362	#N/A	#N/A	30	CXCL3	5.8488598	-1.414918	7.2637783
2	CCL20	7.84118389	-9.0371137	16.87829759	31	CCL11	4.3465385	-1.846978	6.1935169
3	CCL4	7.385725312	-8.121418378	15.50714369	32	CCL13	7.1645523	1.0228712	6.1416811
4	CXCL12	9.362715565	-5.711969811	15.07468538	33	IL8	9.0962637	3.0039511	6.0923126
5	CCL5	9.645948946	-4.542921912	14.18887086	34	CMTM1	6.8196198	0.7604167	6.0592031
6	CMTM7	9.129737689	-4.942406426	14.07214412	35	CXCL9	9.8496959	4.0281311	5.8215648
7	CX3CL1	10.45440596	-3.576200488	14.03060644	36	CCL2	9.5295442	3.9776821	5.5518621
8	CMTM4	10.40824186	-3.612567138	14.020809	37	XCL2	3.4778559	-2.043175	5.5210304
9	CXCL2	8.755947822	-4.767556664	13.52350449	38	CCL21	9.2568421	4.0840485	5.1727936
10	CCL18	10.39373753	-2.776079784	13.16981732	39	PF4V1	-3.101798	1.8816516	4.9834496
11	CKLF	8.982831291	-4.143342964	13.12617425	40	CXCL5	6.7468356	1.9241471	4.8226885
12	CXCL16	11.47948488	-1.360862383	12.84034726	41	CXCL10	8.5552614	4.0402369	4.5150244
13	CXCL17	11.61901907	-0.900788883	12.51980795	42	CCL1	-4.343596	-0.041513	4.3020834
14	CXCL1	8.045495332	-3.737580465	11.7830758	43	CXCL13	7.932574	4.0802832	3.8522908
15	CXCL14	8.963378695	-2.66201104	11.62538973	44	CMTM5	-2.831917	-6.612594	3.7806769

16	TNFSF10	11.10545904	-0.325995977	11.43145502	45	CXCL6	4.251994	0.7457797	3.5062144
17	CCL14	7.121191244	-4.098422478	11.21961372	46	PF4	-0.976833	-4.21609	3.2392575
18	CMTM3	10.03404108	-0.925042308	10.95908339	47	CCL8	5.6036706	2.4283287	3.1753419
19	CCL3	7.22021579	-3.563608469	10.78382426	48	CCL4L2	6.3184124	3.3810569	2.9373555
20	CCL28	5.716015788	-3.664398663	9.380414451	49	CCL24	-0.17963	-2.523985	2.3443544
21	CCL19	7.707818672	-1.456895438	9.164714109	50	CCL23	3.5472646	1.2177978	2.3294668
22	CCL14-CCL15	-4.154368948	4.959097597	9.113466545	51	CXCL11	6.2726911	4.1629949	2.1096962
23	CCL17	4.586962265	-4.472438144	9.05940041	52	CMTM2	1.8933637	3.6230415	1.7296778
24	CMTM6	11.47274262	2.807684539	8.66505808	53	CCL25	-1.386629	-0.013187	1.3734421
25	CMTM8	7.996154788	-0.398715859	8.394870647	54	CCL16	-3.12846	-1.914748	1.2137123
26	XCL1	3.469324468	-4.442123275	7.911447743	55	PPBP	1.9129656	0.7233595	1.189606
27	CCL27	-7.352037039	0.507800707	7.859837745	56	CCL3L3	-1.175233	-2.281442	1.1062088
28	CCL22	7.469620335	-0.121789179	7.591409514	57	CCL15	1.1495801	0.8214712	0.3281089
29	CCL7	2.2115319	-5.250983	7.4625146	58	CCL26	1.080855	0.2412889	0.839566